MOLECULAR AND CELLULAR BIOLOGY, Jan. 2004, p. 200–216 Vol. 24, No. 1
0270-7306/04/$08.00+0 DOI: 10.1128/MCB.24.1.200–216.2004

mTOR Controls Cell Cycle Progression through Its Cell Growth Effectors S6K1 and 4E-BP1/Eukaryotic Translation Initiation Factor 4E

Diane C. Fingar, Celeste J. Richardson, Andrew R. Tee, Lynn Cheatham, Christina Tsou, and John Blenis*

Department of Cell Biology, Harvard Medical School, Boston, Massachusetts 02115

Received 23 June 2003/Returned for modification 25 August 2003/Accepted 29 October 2003

The mammalian target of rapamycin (mTOR) integrates nutrient and mitogen signals to regulate cell growth (increased cell mass and cell size) and cell division. The immunosuppressive drug rapamycin inhibits cell cycle progression via inhibition of mTOR; however, the signaling pathways by which mTOR regulates cell cycle progression have remained poorly defined. Here we demonstrate that restoration of mTOR signaling (by using a rapamycin-resistant mutant of mTOR) rescues rapamycin-inhibited G_1-phase progression, and restoration of signaling along the mTOR-dependent S6K1 or 4E-BP1/eukaryotic translation initiation factor 4E (eIF4E) pathways provides partial rescue. Furthermore, interfering RNA-mediated reduction of S6K1 expression or overexpression of mTOR-insensitive 4E-BP1 isoforms that block eIF4E activity inhibit G_1-phase progression individually and additively. Thus, the activities of both the S6K1 and 4E-BP1/eIF4E pathways are required for and independently mediate mTOR-dependent G_1-phase progression. In addition, overexpression of constitutively active mutants of S6K1 or wild-type eIF4E accelerates serum-stimulated G_1-phase progression, and stable expression of wild-type S6K1 confers a proliferative advantage in low-serum-containing media, suggesting that the activity of each of these pathways is limiting for cell proliferation. These data demonstrate that, as for the regulation of cell growth and cell size, the S6K1 and 4E-BP1/eIF4E pathways each represent critical mediators of mTOR-dependent cell cycle control.

Although cell growth (an increase in cell mass and cell size through macromolecular biosynthesis) and cell division are distinct processes and therefore separable under some conditions (13, 22, 32), they are generally tightly coupled such that cell mass and DNA content double during each cell division cycle. Such a mechanism ensures that appropriately sized daughter cells are produced after mitosis. Although the mechanisms by which cell growth and cell cycle division are coordinated are poorly understood, the signaling protein TOR (for target of rapamycin; also known as FRAP, RAFT, or RAPT in mammals) regulates both cell growth and cell cycle progression in species from yeast to flies to mammals and as such is recognized as an evolutionarily conserved central coordinator of these fundamental biological processes (reviewed in references 9, 19, 34, and 46).

TOR belongs to the phosphatidylinositol kinase-related kinase superfamily in which a lipid kinase homology domain functions as a serine/threonine kinase. When complexed with its cellular receptor FK506-binding protein 12 (FKBP12), the immunosuppressive drug rapamycin directly binds to TOR, resulting in inhibition of TOR-dependent downstream signaling (reviewed in references 15 and 46). Rapamycin treatment induces G_1-phase arrest in yeast cells and mammalian lymphocytes; in most other cell types, however, the drug delays cell cycle progression rather than inducing an absolute block (reviewed in reference 1). Recently, TOR has also been linked to regulation of cell growth. In flies, larvae null for *Drosophila melanogaster* TOR (dTOR) are reduced in size, and dTOR-null cells are reduced in size (35, 61). In mammalian cells, rapamycin reduces cell size, and restoration of mammalian TOR (mTOR) signaling rescues this reduced cell size phenotype (13). Thus, TOR signaling regulates both cell cycle progression and cell growth/cell size.

In yeast, TOR monitors and responds to nutrient levels (reviewed in reference 39). In more complex multicellular organisms, however, TOR integrates signals from both nutrients and growth factors (reviewed in reference 46). How nutrients regulate TOR is poorly understood. A novel positive regulator of TOR, the small GTPase Rheb (named for Ras homologue enriched in brain), has recently been shown to function as an integrator of both nutrient and mitogenic signals (14, 43, 49, 54, 62). The tuberous sclerosis complex proteins TSC1/TSC 2 (hamartin/tuberin) negatively regulate TOR by inactivating Rheb through TSC2's (tuberin's) GTPase activating protein (GAP) activity (14, 54, 62; reviewed in reference 31). Mitogens, through direct phosphorylation of TSC2 (tuberin) by Akt/protein kinase B, inhibit the tumor suppressor function of the tuberous sclerosis complex, thereby indirectly promoting TOR-dependent signaling (reviewed in reference 31).

The best-characterized downstream effectors of mTOR include two signaling pathways that act in parallel to control mRNA translation: the 70-kDa ribosomal protein S6 kinase 1 ($p70^{S6K1}$ or S6K1) pathway and the eukaryotic translation initiation factor 4E (eIF4E)-binding protein 1 (4E-BP1; also known as PHAS-I)/eIF4E pathway. mTOR-dependent signals, in cooperation with phosphatidylinositol 3-kinase-dependent signals, mediate phosphorylation and activation of S6K1 and

* Corresponding author. Mailing address: Department of Cell Biology, Harvard Medical School, 240 Longwood Ave., Boston, MA 02115. Phone: (617) 432-4848. Fax: (617) 432-1144. E-mail: john_blenis@hms.harvard.edu.

phosphorylation and inactivation of 4E-BP1 (a repressor of translation initiation) (reviewed in references 15 and 29). S6K1 directly phosphorylates the 40S ribosomal protein S6, which is thought to increase the translation of mRNA species that possess a 5′-terminal oligopyrimidine (5′-TOP) (20, 21, 56). Since ribosomal proteins and translation elongation factors are encoded by 5′-TOP mRNAs, signaling along the S6K1 pathway may promote ribosome biogenesis and therefore enhance protein biosynthetic capacity, although such a model has been questioned (50, 53).

Hypophosphorylated 4E-BP1 binds to and inhibits the rate-limiting translation initiation factor eIF4E, which binds the cap (m^7GpppN) at the 5′ ends of mRNA transcripts to initiate cap-dependent translation (reviewed in references 15 and 29). A recently identified mTOR-interacting protein, raptor, links mTOR to substrates such as 4E-BP1 (16, 25) by binding to the TOR signaling (TOS) motif in the C terminus of 4E-BP1 (either directly or indirectly), enabling mTOR-dependent phosphorylation of 4E-BP1 in response to nutrients or growth factors (8, 33, 45, 59). Upon phosphorylation, 4E-BP1 releases from eIF4E, allowing eIF4E to assemble with other translation initiation factors to initiate cap-dependent translation. eIF4E is thought to enhance the translation of transcripts possessing either complex 5′-untranslated region (UTR) secondary structure and/or upstream open reading frames, which often encode proteins associated with a proliferative response (reviewed in reference 48).

Although some experiments have suggested a critical role for S6K1 in S-phase progression (26), mice null for S6K1, although slightly smaller than wild-type (WT) littermates at birth, exhibit few abnormalities (47), and S6K1-null embryonic stem cells exhibit only a mild reduction in cell proliferation rate (23). Thus, although S6K1 is generally thought to play a role in cell cycle progression, its contribution relative to other mTOR-mediated signals is unclear. A potential role for 4E-BP1/eIF4E in cell cycle progression has not been carefully investigated, although eIF4E overexpression transforms rodent fibroblasts (27) and is commonly observed to be overexpressed in human tumors (reviewed in reference 51). We therefore investigated the individual roles of S6K1, 4E-BP1, and eIF4E in mammalian cell cycle progression. We previously reported that the S6K1 and eIF4E pathways function independently to increase cell size downstream of mTOR (13). We now report that these pathways each promote mTOR-dependent cell cycle progression and that the activity of each pathway is rate limiting for cell cycle progression in mammalian cells. The function of these biosynthetic pathways as mediators of cell cycle progression is consistent with a role for these pathways in coupling cell growth with cell cycle progression during cell proliferation.

MATERIALS AND METHODS

Materials. Rapamycin was kindly provided by S. N. Seghal (Wyeth). RNase A and Fugene 6 transfection reagent were from Roche, and nitrocellulose membrane was from Schleicher & Schuell. X-ray film was from Kodak (X-OMAT LS). All other chemicals were from Sigma.

Antibodies. Anti-AU1 monoclonal antibodies were from Covance, and anti-CD20-fluorescein isothiocyanate (FITC) monoclonal antibodies were from BD Pharmingen. Antihemagglutin in (anti-HA) monoclonal antibodies were kindly provided by Margaret Chou (University of Pennsylvania, Philadelphia), and anti-phospho-S6 antibodies were generously provided by Morris Birnbaum (University of Pennsylvania and Howard Hughes Medical Institute, Philadelphia). Anti-eIF4E antibodies were from Cell Signaling Technology. Anti-S6K1 (6) and anti-mitogen-activated protein kinase (anti-MAPK) (7) antibodies have been described. Anti-green fluorescent protein (anti-GFP) monoclonal antibodies were from Sigma, and anti-chloramphenicol acetyltransferase (anti-CAT) antibodies were from Cortex Biochem (formerly 5-Prime 3-Prime). For immunoblotting, anti-rabbit and anti-mouse horseradish peroxidase-conjugated secondary antibodies were from Amersham and Chemicon, respectively.

Plasmids. pcDNA3/AU1-mTOR eukaryotic expression plasmids encoding WT, rapamycin-resistant (RR; Ser2035Ile), kinase-dead (KD; Asp2338Ala), and double RR/KD alleles of rat mTOR were kindly provided by Robert Abraham (Burnham Institute, San Diego, Calif.) and have been described elsewhere (5). pRK7/HA-S6K1 eukaryotic expression plasmids encoding WT and KD (Lys100Arg) alleles of rat S6K1 (αII) have been described previously (6). The two partial rapamycin-resistant mutants of S6K1, $E_{389}D_3E$ (37) and $E_{389}\Delta CT$ (44), have been described. $E_{389}D_3E$, containing the point mutations T389E, S411D, S418D, T421E, and S424D, was generated in this lab but was originally described elsewhere (37). pCMV/CD20 was provided by Ed Harlow (Harvard Medical School, Boston, Mass.), and the bicistronic plasmid pGFP/CAT was provided by A. A. M. Thomas (University of Utrecht). The plasmids pMV7/3HA-eIF4E, pACTAG2/HA-WT-4E-BP1, and pACTAG2/HA-AA-4E-BP1 (Thr37/46Ala) were generously provided by Nahum Sonenberg (McGill University, Montreal, Quebec, Canada). Plasmid pACTAG2/3HA-F114A-4E-BP1 has been described (44), and pACTAG2/3HA-AA-Y54A-4E-BP1 (Thr37/46Ala; Tyr54Ala) was generated by using QuickChange (Stratagene) with the AA-4E-BP1 plasmid as a template. pRK7/3HA-eIF4E was generated by PCR amplifying 3HA-eIF4E from pMV7 and subcloning it into pRK7. The hairpin interfering RNA (RNAi) plasmid targeting S6K1 (pBS/U6-S6K1) was generated as follows. The sequence below (the sense strand only is shown) was cloned into pBS/U6 (52) between the *Apa*I and *Eco*RI restriction sites to express hairpin RNA from the U6 promoter. In boldface is the targeting DNA sequence (nucleotides 284 to 304 of human S6K1): 5′-**GGGTACTTGGTAAAGGGGGCT**TTCAAGCTTAGCCCCCTTTACCAAGTACCCTTTTT-3′.

Cell culture and transfection. Human U2OS osteosarcoma cells were cultured at 37°C and 5% CO_2 in Dulbecco modified Eagle medium (DMEM)–10% fetal bovine serum (FBS). A total of 1.5×10^5 cells were seeded onto 60-mm plates and then transfected 24 h later with Fugene 6 overnight according to the manufacturer's directions by using 5 to 10 μg of total DNA, depending on the experiment. Cells were then washed once with DMEM, deprived of serum for 30 h (DMEM plus 20 mM HEPES [pH 7.2]), and refed with DMEM–10% FBS in the absence or presence of rapamycin at 20 ng/ml for 20 h unless otherwise noted.

Cell lysis and immunoblotting. Cells were washed once with ice-cold STE (pH 7.2; 150 mM NaCl, 50 mM Tris-HCl, 1 mM EDTA), scraped in lysis buffer (pH 7.2; 10 mM KPO_4, 1 mM EDTA, 10 mM $MgCl_2$, 50 mM β-glycerophosphate, 5 mM EGTA, 0.5% NP-40, 0.1% Brij-35, 1 mM sodium orthovanadate, 40 μg of phenylmethylsulfonyl fluoride/ml, 10 μg of leupeptin/ml, 5 μg of pepstatin A/ml), and spun at 15,000 rpm for 5 min. Lysates were subjected to sodium dodecyl sulfate-polyacrylamide gel electrophoresis (SDS-PAGE), transferred to nitrocellulose membrane, immunoblotted with primary antibodies followed by horseradish peroxidase-conjugated secondary antibodies, and developed via enhanced chemiluminescence. A Bradford assay was used to determine the protein content (Bio-Rad).

Immunoprecipitations and immune complex kinase assays. Cell extracts were immunoprecipitated with anti-HA antibodies for 2 h, followed by incubation with protein A-Sepharose CL4B (Pharmacia) for 1 h. Immunoprecipitates were washed with 1 ml each of ice-cold buffer A, buffer B, and buffer ST (salt-Tris) as described previously (30). The kinase activity in washed immunoprecipitates was assayed with recombinant GST-S6 (32 C-terminal amino acids of ribosomal protein S6) as in vitro substrate, as described previously (30). The amount of ^{32}P incorporated into glutathione *S*-transferase (GST)–S6 was assessed by autoradiography and quantitated on a Bio-Rad phosphorimager with ImageQuant software.

Indirect immunofluorescence. U2OS cells were plated to glass coverslips in 35-mm wells at 0.5×10^5 cells/well and cotransfected 24 h later with Fugene 6 with 0.2 μg of pCMV/CD20 and 2.0 μg of pBS/U6 or pBS/U6-S6K1. After overnight transfection, the cells were serum deprived for 30 h and refed with DMEM–10% FBS for 20 h. Coverslips were washed twice in 2 ml of phosphate-buffered saline plus Ca and Mg ($PBS^{+Ca/Mg}$), incubated in anti-CD20-FITC antibodies diluted 1:10 in $PBS^{+Ca/Mg}$ 30 min, washed twice in $PBS^{+Ca/Mg}$, and then fixed 10 min in 3.7% formaldehyde (Polysciences, Inc.) in $PBS^{+Ca/Mg}$. After fixation, the coverslips were washed, blocked and/or permeabilized for 30 min in $PBS^{+Ca/Mg}$–0.2% fish skin gelatin (FSG)–0.2% Triton X-100 (TX-100), and

incubated for 30 min with anti-phospho-S6 antibodies diluted 1:500 in $PBS^{+Ca/Mg}$–FSG–TX-100. Coverslips were then washed, incubated for 30 min in donkey anti-rabbit Texas red (1:500; Jackson Laboratories) in $PBS^{+Ca/Mg}$–FSG–TX-100, washed once in $PBS^{+Ca/Mg}$–FSG plus DAPI (4′,6′-diamidino-2-phenylindole) at 0.1 μg/ml, washed twice in $PBS^{+Ca/Mg}$–FSG and twice in $PBS^{+Ca/Mg}$, dipped in distilled H_2O, mounted on CitiFluor (Ted Pella), and finally sealed with nail polish. Immunofluorescence images were acquired by using a Nikon Eclipse E800 upright epifluorescence microscope equipped with an Orca 100 camera and Metamorph software.

m^7GTP cap-binding assays. Cell extracts were incubated in 20 μl of 7-methyl GTP-Sepharose 4B (Amersham Pharmacia) for 2 h at 4°C and then washed twice in lysis buffer. Sepharose beads were resuspended in Laemmli sample buffer with 2% β-mercaptoethanol and resolved by SDS-PAGE.

Cap-dependent translation assay. U2OS cells were cotransfected with 0.5 μg of pACTAG2/3HA-4E-BP1 plasmids and 5 μg of the bicistronic plasmid pGFP/CAT, serum deprived for 30 h, and refed with DMEM–10% FBS in the absence or presence of rapamycin for 20 h. [^{35}S]methionine-cysteine (Translabel; ICN) at 0.25 mCi/ml was included during the last 2 h of serum deprivation or the last 2 h of FBS stimulation. After preparation of cell extracts, GFP and CAT proteins were immunoprecipitated with a mixture of anti-GFP and anti-CAT antibodies, which were then resolved on a SDS–12% polyacrylamide gel. After electrophoresis, the gel was stained, fixed, incubated in 1 M sodium salicylate (pH 6.0) for 30 min, dried, and exposed to X-ray film. The ratio of GFP to CAT was determined by autoradiography and quantification of ^{35}S bands on a Bio-Rad phosphorimager by using ImageQuant software.

Flow cytometry. To determine DNA content, a Becton Dickinson FACSCalibur flow cytometer with CellQuest software was used. U2OS cells were seeded to 60-mm dishes at 1.5×10^5 cells/plate and transfected in triplicate the next day with 1 μg of CD20 and 10 μg of total plasmid to be assayed. After overnight transfection, followed by serum deprivation and stimulation (as described above), cells were harvested for analysis by flow cytometry as described earlier (13). Briefly, cells were removed from the plates with PBS–EDTA, incubated with anti-CD20-FITC antibodies, fixed in ethanol (80% final), and then incubated in propidium iodide-RNase A. To determine the DNA content of the untransfected cell population, 10,000 propidium iodide$^+$ FITC$^-$ cells were collected. To determine the DNA content of the transfected cell population, 3,000 to 5,000 propidium iodide$^+$ FITC$^+$ cells were collected. Single cells were gated away from clumped cells by using an FL2 width versus FL-2 area dot plot. To quantitatively measure the percentage of cells in the various phases of the cell cycle, the marker tool within CellQuest was used to specifically gate on the G_0/G_1-, S-, and G_2/M-phase peaks within an FL2 area histogram. All cell cycle data represent the means ± the standard deviations of triplicate transfections unless otherwise noted.

Generation of stable C2C12 cell lines and proliferation assay. C2C12 myoblasts were cultured in DMEM–20% FBS and 5% CO_2. To generate stable cell lines expressing exogenous HA-tagged S6K1, cells were infected with an S6K1-expressing retrovirus or with a pMV7 control virus and selected in G418. Pools of G418-resistant colonies were collected. To measure the ability of these cell lines to proliferate in low-serum-containing media (i.e., media containing low levels of serum), 10^4 cells were seeded into triplicate 35-mm wells directly in DMEM–2% FBS and then incubated for 2, 4, 5, and 6 days in this medium. The cell number was determined by counting the cells with a hemocytometer.

Statistical analysis. Data are presented as the means ± the standard deviations. The statistical significance was determined by using the Student *t* test (paired two sample for means; two tails) by using Microsoft Excel. *P* values of <0.05 were considered significant.

RESULTS

RR mTOR (RR-mTOR) rescues the inhibitory effect of rapamycin on G_0-to-S-phase cell cycle progression. While the mTOR inhibitor rapamycin is known to block G_1-phase progression, the biochemical signaling pathways regulated by mTOR to control cell cycle progression are poorly defined. We thus set out to investigate the role(s) of the S6K1 and 4E-BP1/eIF4E pathways in cell cycle progression, which also mediate mTOR-dependent cell growth and cell size (13). We chose to perform our analysis in human osteosarcoma U2OS cells, since they are readily synchronized and amenable to transfection. After serum deprivation for 30 h to synchronize the cells in G_0 phase, U2OS cells were stimulated with serum in the absence or presence of rapamycin for various times, and DNA content and/or cell cycle profiles were determined by flow cytometry of propidium iodide-stained cells (Fig. 1). This analysis demonstrated that U2OS cells began entering S phase at between 12 and 16 h of serum stimulation and that rapamycin delayed entry into S phase by about 8 h.

Although TOR was initially identified as a gene that, when mutated in budding yeast, conferred resistance to the antiproliferative action of rapamycin (18), the mTOR-dependent nature of the rapamycin-induced effects on cell cycle progression and cellular proliferation in mammalian cells has not been formally demonstrated. We thus assayed the ability of RR-mTOR to rescue rapamycin-inhibited cell cycle progression in U2OS cells. Cells were transiently cotransfected with the cell surface marker CD20 and cDNAs for various mTOR isoforms, serum starved, and stimulated with serum for 20 h in the absence or presence of rapamycin. We chose the 20-h time point for this analysis since there is a marked difference in the percentage of cells that have entered S phase in the absence or presence of drug at this time (Fig. 1). To determine DNA content, cells were stained with anti-CD20-FITC-conjugated antibodies and propidium iodide and then analyzed on a flow cytometer. As expected, expression of RR-mTOR rescued G_0-to-S-phase cell cycle progression in the presence of rapamycin, whereas the double RR/KD mutant did not, indicating that inhibition of mTOR is the mechanism by which rapamycin delays cell cycle progression and that the kinase activity of mTOR is required for rescue (Fig. 2A and B). Importantly, only the FITC$^+$ cells transfected with RR-mTOR (Fig. 2B) (which represent a population enriched in transfected cells) and not the FITC$^-$ cells (Fig. 2C) (which represent a population enriched in untransfected cells) displayed rescue of rapamycin-inhibited cell cycle progression, and all four mTOR constructs were expressed to similar levels (Fig. 2D). Interestingly, although neither of the mTOR mutants containing the kinase-inactivating mutation (RR/KD or KD) inhibited G_1-phase progression in a dominant-negative manner in the absence of rapamycin, both potentiated the inhibitory effect of rapamycin on S-phase entry.

To confirm that expression of RR-mTOR allows signaling to two of its major downstream targets in the presence of rapamycin in this experimental context, we cotransfected U2OS cells with various mTOR plasmids together with either HA-tagged S6K1 (Fig. 2E) or HA-tagged 4E-BP1 (Fig. 2F). As reported previously (4), RR-mTOR rescued the inhibitory effect of rapamycin on S6K1 activity, as assayed by mobility shift (anti-HA blot), anti-phospho-S6 immunoblotting, and in vitro kinase assay with recombinant GST-S6 as substrate (Fig. 2E). Expression of KD-mTOR decreased S6K1 activity slightly in the absence of rapamycin compared to S6K1 activity in WT-mTOR-transfected cells. Since the inhibition of S6K1 activity by rapamycin is complete, no enhanced inhibition by KD-mTOR could be detected.

RR-mTOR also rescued the inhibitory effect of rapamycin on 4E-BP1 phosphorylation, as determined by anti-HA mobility shift (Fig. 2F), a finding consistent with published results (5, 17). As observed for S6K1 inhibition, the expression of KD-mTOR constructs in the absence of rapamycin produced a dominant-negative effect and increased the intensity of the

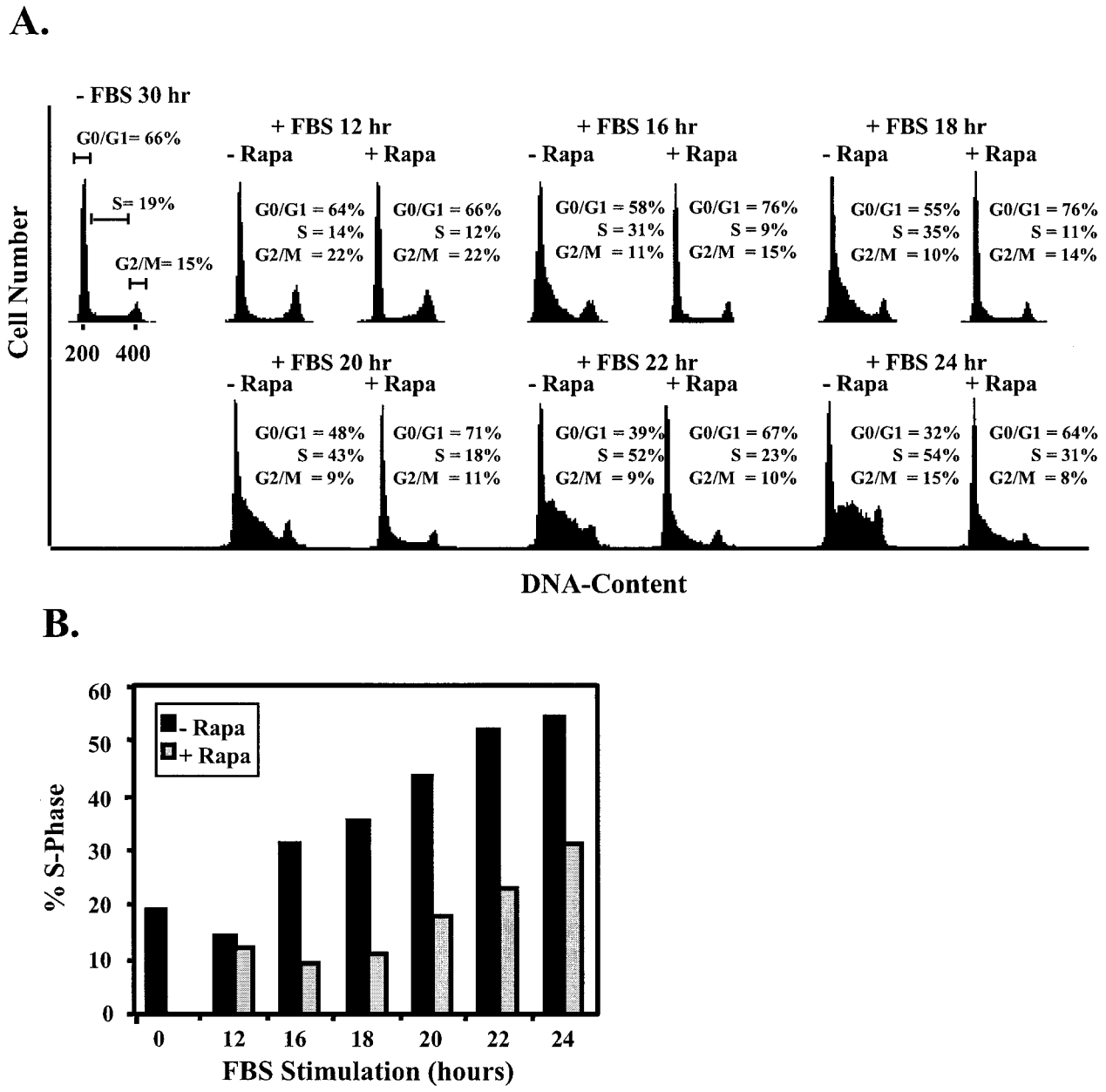

FIG. 1. Rapamycin delays G_1-phase progression in U2OS cells. U2OS cells were serum deprived for 30 h and then refed with DMEM–10% FBS for the indicated time points between 12 and 24 h in the absence (−Rapa) or presence (+Rapa) of rapamycin at 20 ng/ml. DNA content was determined on a flow cytometer. DNA content histograms are shown in panel A with the percentage of cells in each cell cycle phase indicated. Propidium iodide positive staining is graphed on the *x* axis with cell number on the *y* axis. Quantitation of the percentage of cells that have entered S phase at the various time points is shown graphically in panel B.

hypophosphorylated α-band, a finding consistent with decreased 4EBP1 phosphorylation (Fig. 2F, short exposure). As for cell cycle progression, KD constructs also potentiated the inhibitory effect of rapamycin on 4EBP1 phosphorylation (Fig. 2F, long exposure). The further decrease in 4EBP1 phosphorylation and cell cycle progression by KD-mTOR isoforms in the presence of rapamycin is consistent with some level of rapamycin-insensitive signaling by mTOR.

Activation of S6K1 partially rescues the inhibitory effect of rapamycin on G_1-phase progression and accelerates G_1 progression in the absence of drug. To link the S6K1 pathway to mTOR-dependent cell cycle progression, we sought to determine whether expression of RR mutants of S6K1 could rescue cell cycle progression in the presence of rapamycin. U2OS cells were transfected with a panel of S6K1 plasmids, serum deprived, stimulated in the absence or presence of rapamycin, and analyzed by flow cytometry to determine DNA content (Fig. 3A). Rapamycin inhibited S-phase entry, as expected, whereas cells expressing two different RR-S6K1 constructs ($E_{389}D_3E$ and $E_{389}\Delta CT$) displayed modest but significantly

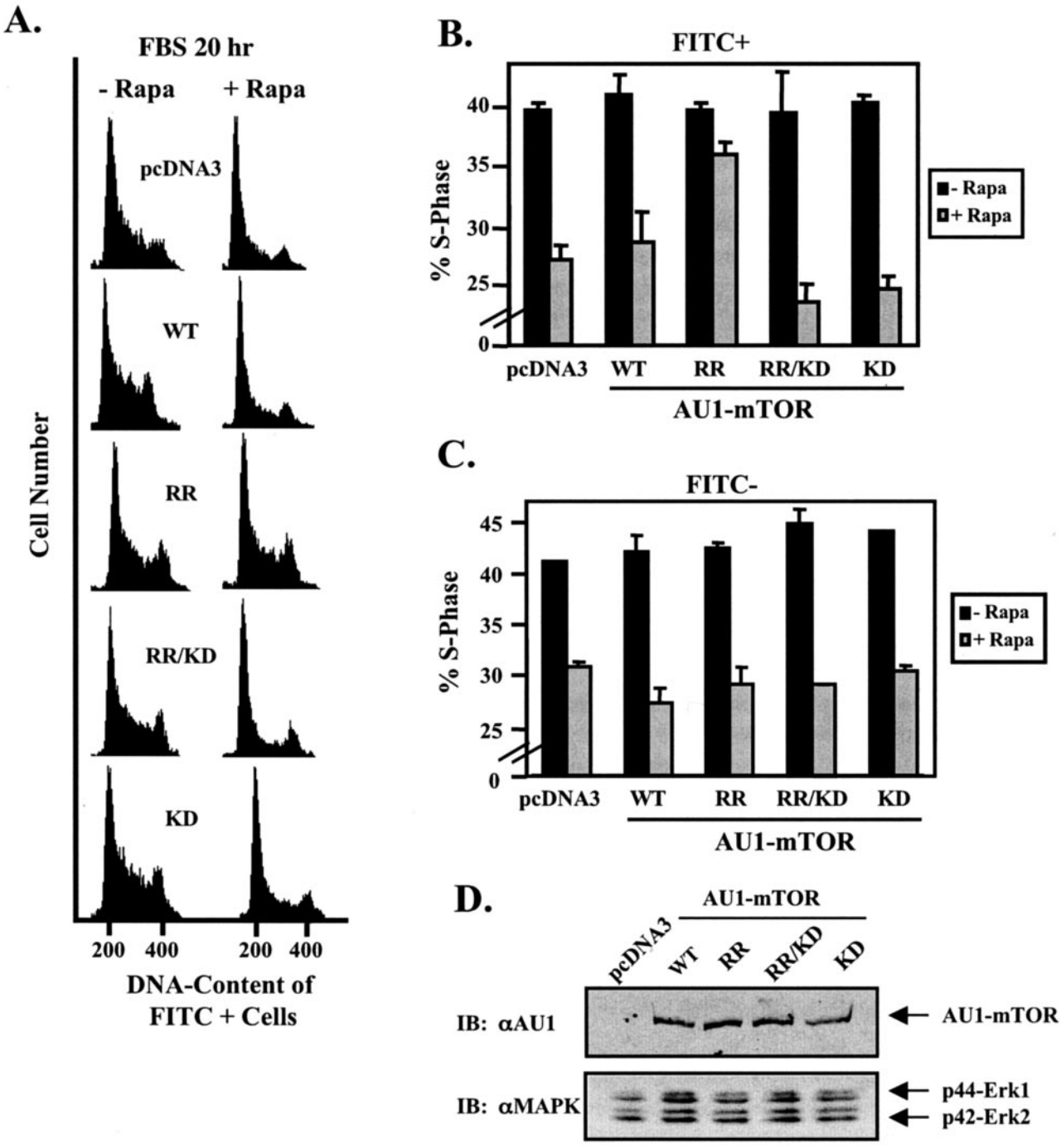

FIG. 2. RR-mTOR rescues rapamycin-inhibited G_1-phase progression. U2OS cells were transiently cotransfected with CD20 (1 μg) and various mTOR plasmids or pcDNA3 vector control (10 μg). After overnight incubation, cells were serum deprived, as described above, refed with DMEM–10% FBS for 20 h in the absence or presence of rapamycin, and analyzed on a flow cytometer. DNA content histograms of the $FITC^+$ cells are shown in panel A. The percentage of $FITC^+$ (B) and $FITC^-$ (C) cells that have entered S phase after 20 h serum stimulation is shown. (D) Protein expression levels of transfected mTOR constructs in this experiment were assayed by anti-AU1 immunoblotting. An anti-MAPK immunoblot is shown to control for protein loading. (E) In order to show that RR-mTOR rescues rapamycin-inhibited S6K1 signaling, cells were cotransfected with a panel of AU1-tagged mTOR constructs (10 μg) and HA-tagged S6K1 (1 μg). Cells were serum deprived, refed with DMEM–10% FBS in the absence or presence of rapamycin, lysed, and analyzed by anti-AU1, anti-HA, anti-MAPK, and anti-phospho-S6 immunoblotting. The activity of cotransfected S6K1 was assayed by anti-HA immune complex kinase assay using recombinant GST-S6 as in vitro substrate. (F) In order to show that RR-mTOR rescues rapamycin-inhibited 4E-BP1 phosphorylation, cells were cotransfected with a panel of AU1-tagged mTOR constructs (10 μg) and HA-tagged 4E-BP1 (1 μg). Cells were then serum deprived, refed with DMEM–10% FBS in the absence or presence of rapamycin, lysed, and analyzed by anti-AU1, anti-HA, and anti-MAPK immunoblotting. Short and long anti-HA immunoblot exposures are shown as indicated. The most hypophosphorylated 4E-BP1 species is marked α, the most hyperphosphorylated species is marked γ, and the band representing an intermediate phosphorylation state is marked β.

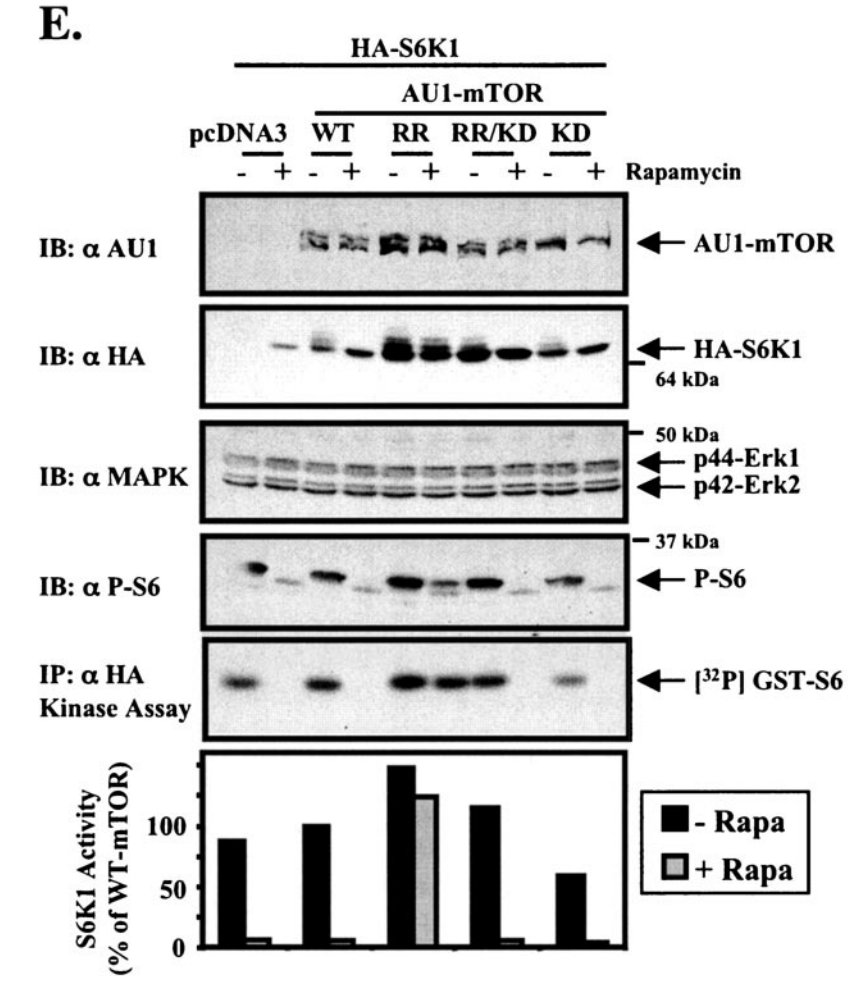

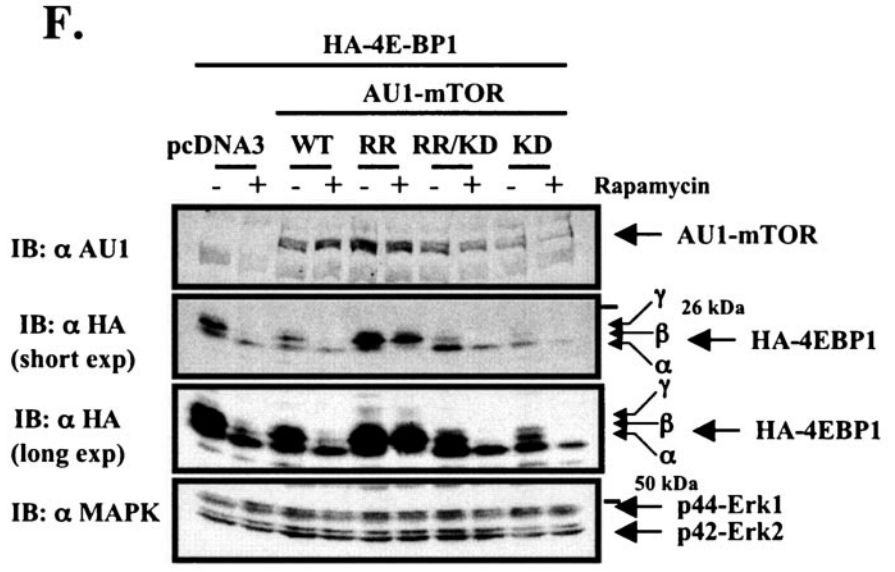

FIG. 2—*Continued*.

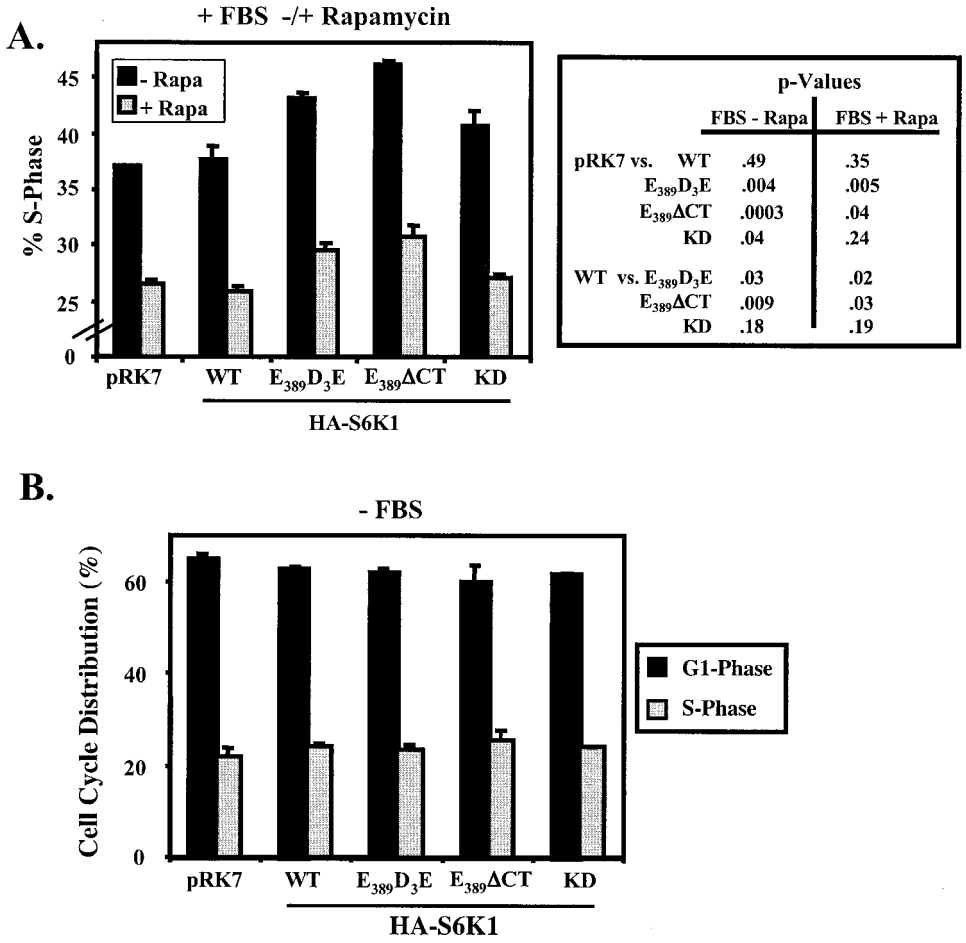

FIG. 3. RR-S6K1 partially rescues rapamycin-inhibited G_1-phase progression and accelerates G_1-phase progression in the absence of drug. (A) U2OS cells were transiently cotransfected with CD20 (1 μg) and various HA-tagged S6K1 plasmids or pRK7 vector control (10 μg). Cells were then serum deprived, refed with DMEM–10% FBS for 20 h in the absence or presence of rapamycin, and analyzed on a flow cytometer. The percentage of $FITC^+$ (transfected) cells that have entered S phase after 20 h serum stimulation is shown. *P* values to determine statistical significance for various comparisons are shown in the table to the right. When $FITC^-$ (untransfected) cells were analyzed (data not shown), there were no statistically significant differences. (B) The percentage of cells in G_1 and S phase after 30 h serum deprivation is shown. (C) To determine the rapamycin-resistant activity displayed by two different RR-S6K1 constructs, cells were transiently transfected with a panel of HA-tagged S6K1 constructs (5 μg), serum deprived, and refed with media containing10% FBS in the absence or presence of rapamycin. Lysates were immunoblotted with anti-HA and anti-phospho-S6 antibodies. Kinase activity was determined by anti-HA immune complex kinase assay. (D) The kinase activity of transfected HA-S6K1-transfected cells after 30 h serum deprivation was determined by immune complex kinase assay as described above. Lysates were also immunoblotted with anti-HA, anti-MAPK (loading control), and anti-phospho-S6 antibodies.

enhanced S-phase entry in the presence of rapamycin compared to the vector control and WT- or KD-S6K1-transfected cells (see Fig. 3A for *P* values). Furthermore, cells expressing the two partially rapamycin-resistant mutants of S6K1 ($E_{389}D_3E$ and $E_{389}\Delta CT$) also exhibited modest but significant acceleration of S-phase entry in the absence of rapamycin compared to the vector control and WT- or KD-S6K1-transfected cells (Fig. 3A). When DNA content was determined after serum deprivation, cells expressing the RR-S6K1 constructs displayed cell cycle profiles similar to pRK7- or WT-S6K1-transfected cells, indicating that S-phase entry in cells expressing the RR-S6K1s is not accelerated due to reduced quiescence in G_0 phase (Fig. 3B). The rescue of rapamycin-inhibited G_1-phase progression and the acceleration of G_1-phase progression in the absence of drug upon expression of RR-S6K1 constructs demonstrates that the S6K1 pathway controls G_1-phase cell cycle progression downstream of mTOR. The inability of the RR-S6K1 constructs to completely rescue rapamycin-inhibited cell cycle progression is likely due to the limited resistance of these mutants to rapamycin in U2OS cells (Fig. 3C) combined with the contribution of other mTOR-dependent pathways to cell cycle control.

Since the activity of the RR-S6K1 mutants was similar to WT-S6K1 when they were assayed after 20 h of serum stimulation, as was the extent of phosphorylation of ribosomal protein S6 (Fig. 3C), it was interesting that only the RR-S6K1 mutants accelerated serum-stimulated S-phase entry, whereas WT-S6K1 did not. It is important to note that such mutants are known to possess elevated basal kinase activity. We therefore determined whether these mutants ($E_{389}D_3E$ and $E_{389}\Delta CT$) exhibit elevated kinase activity after serum deprivation in our cell system (Fig. 3D). As expected, the RR-S6K1 mutants

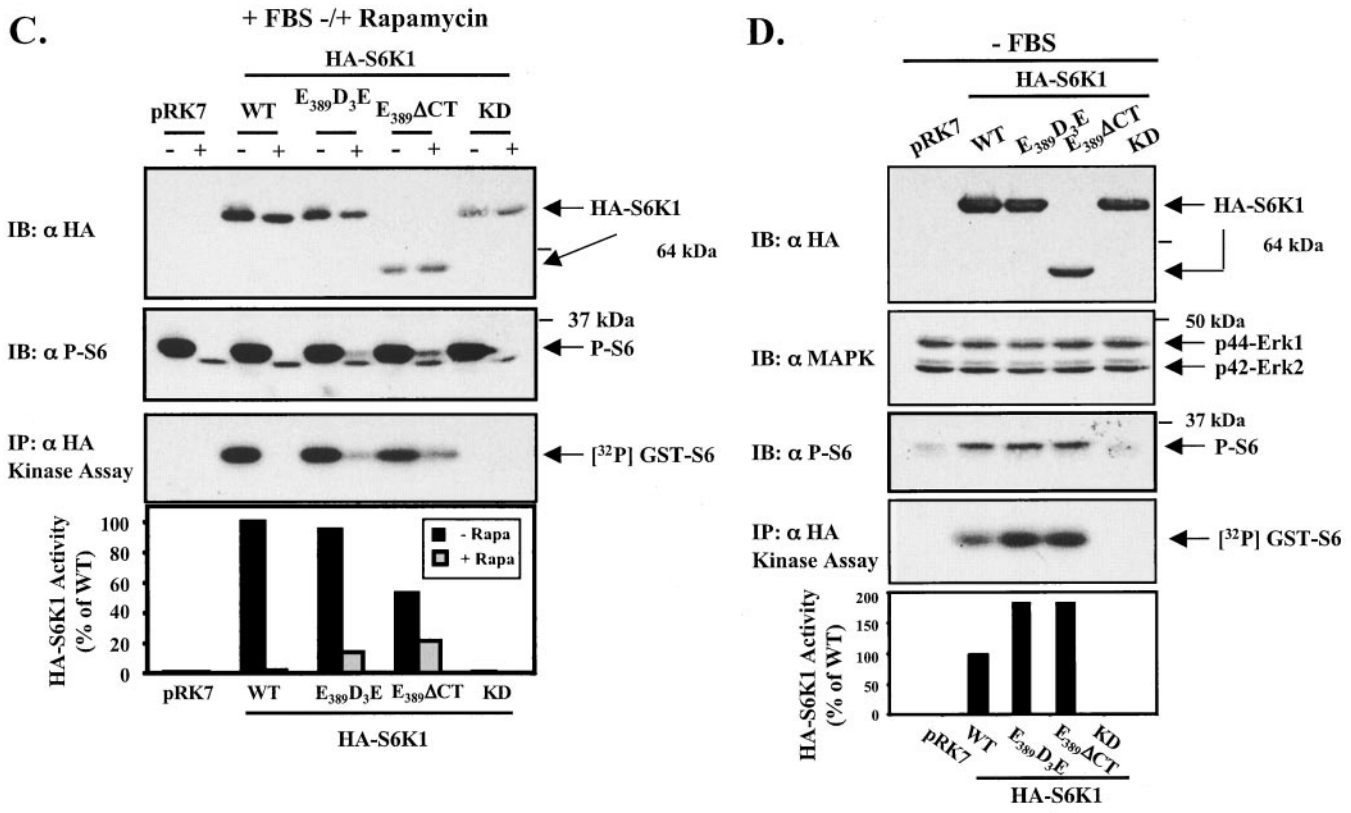

FIG. 3—*Continued*.

possessed increased kinase activity (~2-fold) compared to WT-S6K1 after serum deprivation. These data suggest that cells expressing these "constitutively active" mutants of S6K1 mutants accelerate G_1-phase progression because they have increased kinase activity at $t = 0$ and, as a result, are able to progress through G_1 phase and enter S phase at a faster rate. We also noted that, although overexpression of WT-S6K1 was not sufficient to drive G_1-phase progression, it was sufficient to increase the phosphorylation of endogenous ribosomal protein S6 compared to pRK7 vector control in the absence of serum. Also, whereas $E_{389}D_3E$ and $E_{389}\Delta CT$ accelerated S-phase entry while WT-S6K1 did not, all three S6K1 isoforms increased the phosphorylation state of ribosomal protein S6 to a similar extent over controls after serum deprivation (Fig. 3D), suggesting that perhaps S6K1-dependent phosphorylation of ribosomal protein S6 may not be the critical downstream target of S6K1 for cell cycle control.

RNAi-mediated reduction of S6K1 expression inhibits G_1-phase progression. The data presented above indicate that increased S6K1-dependent signaling is sufficient to accelerate G_1-phase progression downstream of mTOR. To determine whether S6K1-dependent signaling is required for G_1-phase progression, we reduced the expression of S6K1 by using a plasmid-based RNAi approach (52). A hairpin DNA sequence targeting human S6K1 was subcloned into the RNAi vector pBS/U6 to create pBS/U6-S6K1. We first tested whether this hairpin RNAi plasmid could knock down the expression of transfected, exogenous S6K1. To do this, HA-tagged rat S6K1 was cotransfected with pBS/U6 or pBS/U6-S6K1 at various ratios (Fig. 4A; human and rat S6K1 are identical in sequence in the targeted region). A 100:1 ratio of RNAi plasmid to transfected HA-S6K1 resulted in almost complete elimination of exogenous S6K1 expression. To confirm that the hairpin RNAi plasmid could also knock down the expression of endogenous S6K1, we performed immunofluorescence with anti-phospho-S6 antibodies as an indirect measure of endogenous S6K1 activity (we have not been able to identify anti-S6K1 antibodies that specifically detect endogenous S6K1 by immunofluorescence). To identify transfected cells, CD20 and either pBS/U6 or pBS/U6-S6K1 were cotransfected, and the cells were stained with anti-CD20 and anti-phospho-S6 antibodies (Fig. 4B). Cells transfected with the hairpin RNAi plasmid targeting S6K1 exhibited decreased anti-phospho-S6 staining, whereas those transfected with vector control displayed no reduction in anti-phospho-S6 signal. Therefore, the hairpin RNAi plasmid against S6K1 is able to reduce the expression of exogenous S6K1 and reduce the activity of endogenous S6K1. To determine whether S6K1 activity is required for G_1-phase cell cycle progression, either vector control or RNAi-S6K1 plasmids were cotransfected with CD20, and the percentage of cells in S-phase after serum deprivation (−FBS) or after serum stimulation (+FBS) was determined (Fig. 4C). Expression of the RNAi-S6K1 plasmid partially inhibited serum-stimulated S-phase entry, indicating that S6K1 is required for G_1-phase progression. The inability of RNAi-mediated reduction of S6K1 expression to completely block S-phase entry suggests that additional mTOR-dependent signaling pathways also contribute to cell cycle control.

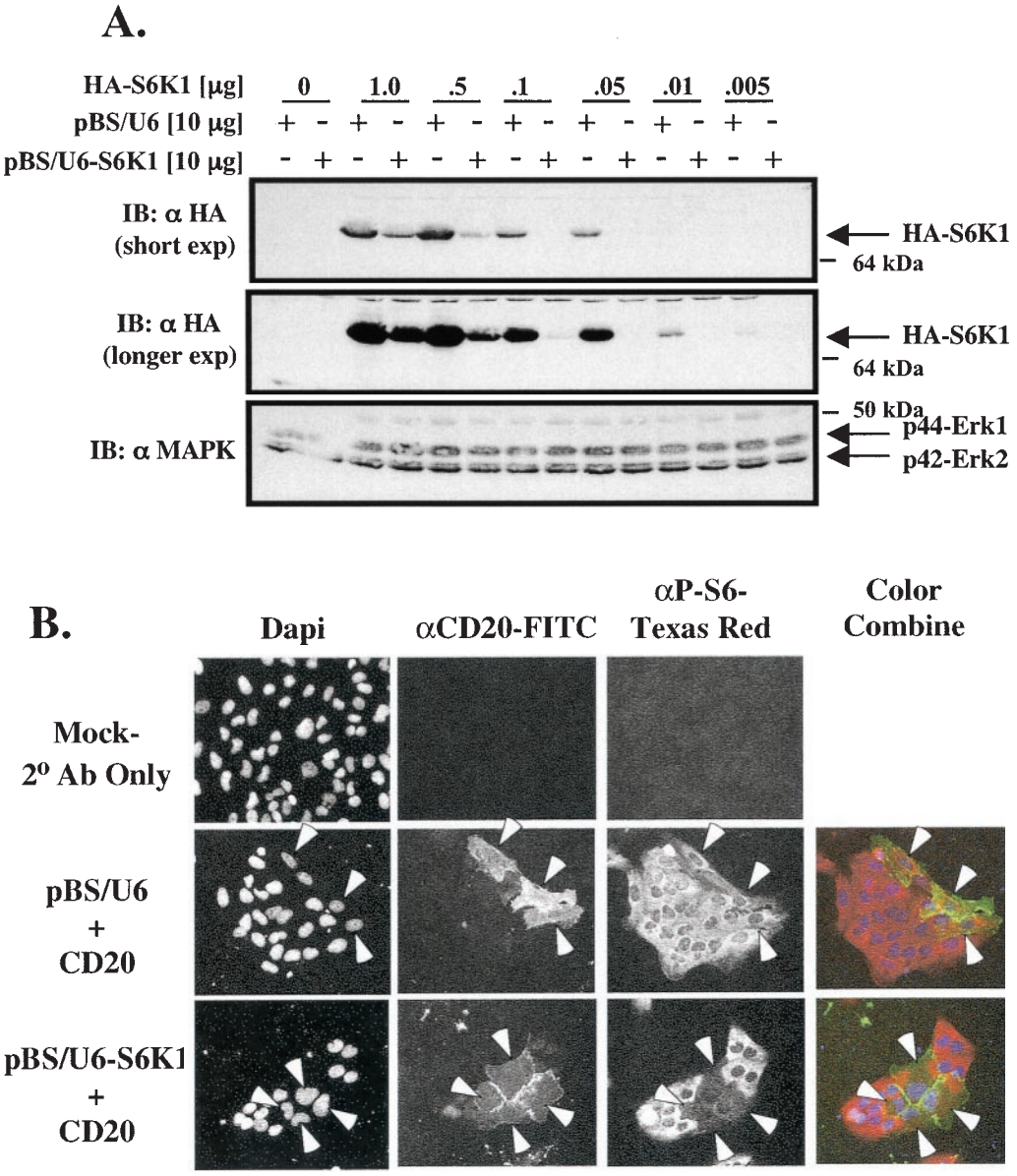

FIG. 4. Reduction of S6K1 expression with plasmid-based RNAi inhibits G_1-phase progression. (A) Cells were cotransfected with 10 μg of either pBS/U6 (RNAi vector) or pBS/U6-S6K1 (which expresses hairpin RNA that targets S6K1), together with various amounts of HA-tagged S6K1. After overnight transfection, cells were serum deprived, refed with DMEM–10% FBS for 20 h, and lysed. Lysates were immunoblotted with anti-HA and anti-MAPK (loading control) antibodies. Short and long anti-HA immunoblot exposures are shown as indicated. (B) Cells were cotransfected on coverslips with either CD20 (0.2 μg) and 2 μg of pBS/U6 (RNAi vector) or pBS/U6-S6K1 (S6K1-RNAi), serum deprived, refed with DMEM–10% FBS for 20 h, and processed for indirect immunofluorescence with anti-CD20 antibodies conjugated to FITC (green), anti-phospho-S6 antibodies, followed by anti-rabbit Texas red secondary antibodies (red), and DAPI to stain the nucleus (blue). Cells cotransfected with CD20 ($FITC^+$) and either pBS/U6 (three cells) or pBS/US-S6K1 (four cells) are marked with open arrowheads. (C) Cells were cotransfected with CD20 (1 μg) and either pBS/U6 (−) or pBS/U6-S6K1 (+) (10 μg), serum deprived, refed where indicated with DMEM–10% FBS for 20 h in the absence or presence of rapamycin, and analyzed on a flow cytometer. The percentages of $FITC^+$ cells in S phase after serum deprivation (−FBS) and of cells that have entered S phase after 20 h of stimulation (+FBS) are shown.

Overexpression of eIF4E partially rescues rapamycin-inhibited G_1-phase progression and accelerates G_1-phase progression in the absence of drug. In order to link the 4E-BP1/eIF4E pathway to mTOR-dependent cell cycle progression, we determined whether overexpression of eIF4E could drive cell cycle progression in the presence of rapamycin. Since overexpression of eIF4E would be expected to overwhelm endogenous 4E-BP1 and render eIF4E constitutively free even in the presence of hypophosphorylated 4E-BP1, overexpression of WT eIF4E seemed to be a reasonable approach to augment eIF4E function. Cells were transfected with pMV7 vector or eIF4E, deprived of serum, stimulated in the absence or presence of rapamycin, and analyzed by flow cytometry (Fig. 5A). Rapamycin inhibited S-phase entry of vector-transfected cells, as

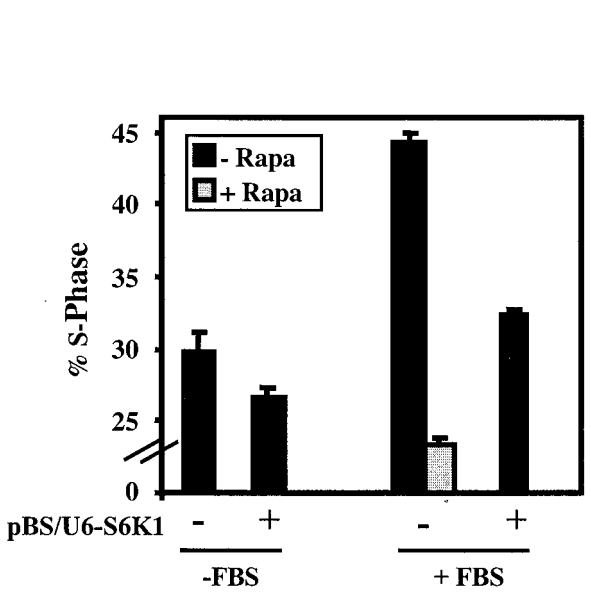

FIG. 4—*Continued*.

expected. Similar to cells expressing RR-S6K1, cells overexpressing eIF4E displayed a small but significant acceleration of S-phase entry in the presence of rapamycin compared to the vector control. As observed in cells expressing constitutively active mutants of S6K1 (Fig. 3A), cells overexpressing eIF4E also showed modest but significant acceleration of G_1-phase progression from G_0 phase to S phase in the absence of rapamycin. Importantly, the eIF4E-expressing cells quiesced similarly to vector control (−FBS) (Fig. 5A). Therefore, the eIF4E pathway mediates a component of mTOR-dependent cell cycle control, similar to what was observed with S6K1.

eIF4E overexpression has been reported to activate a negative-feedback loop that results in dephosphorylation of 4E-BP1 and S6K1 (24), a finding that conflicts with our observation that eIF4E accelerates cell cycle progression. On the other hand, eIF4E overexpression has also been reported to transform rodent fibroblasts (27), which is consistent with our results. We therefore sought to determine whether expression level of exogenous eIF4E could account for this discrepancy by highly overexpressing eIF4E from a strong cytomegalovirus (CMV) promoter (vector pRK7) and determining its effect on cell cycle progression. eIF4E expressed from pRK7 expresses to much higher levels than when expressed from the weak retroviral long terminal repeat promoter (vector pMV7), and significantly more eIF4E binds to m^7GTP beads when expressed from pRK7 than when expressed from pMV7 (Fig. 5B). Importantly, in our cell system, when vastly overexpressed from pRK7, eIF4E inhibits G_1-phase progression (Fig. 5C), a finding consistent with activation of the previously reported negative feedback loop (24).

Overexpression of 4E-BP1 mutants that dominantly inhibit eIF4E partially inhibit G_1-phase progression. In order to eliminate the possibility that the eIF4E phenotypes observed above were the result of an mTOR-independent mechanism, we investigated the role of 4E-BP1 in cell cycle progression. We took advantage of two different mTOR-insensitive mutants of 4E-BP1 that dominantly bind to and constitutively inhibit eIF4E and therefore cap-dependent translation. AA-4E-BP1 contains alanine substitution mutations at threonines 37 and 46, which are mTOR-dependent priming phosphorylation sites, and thus cannot be phosphorylated by mTOR (reviewed in references 15 and 29). F114A-4E-BP1 contains a mutation in the TOS motif and does not associate with the mTOR/raptor complex; consequently, F114A-4E-BP1 cannot be phosphorylated (8, 33, 45, 59). After serum stimulation, expression of WT-4EBP1 exhibited very little inhibitory effect on S-phase entry, whereas AA-4EBP1 significantly inhibited S-phase entry (Fig. 6A). Importantly, this effect on S-phase entry was specific for eIF4E since the AA-Y54A mutant of 4EBP1, which cannot bind eIF4E, failed to inhibit S-phase entry. Overexpression of F114A-4E-BP1 inhibited G_0-to-S-phase progression to a similar extent as the phosphorylation site mutant AA-4E-BP1 (Fig. 6B). These results show that the effects of eIF4E on cell cycle progression described above are mTOR-dependent and demonstrate that mTOR-dependent phosphorylation of 4E-BP1 and mTOR/raptor association with 4E-BP1 is required for mTOR-dependent G_1-phase progression.

To confirm that these 4E-BP1 constructs behave as expected in our cell system, we assayed the ability of the various 4E-BP1 constructs to bind eIF4E in the absence (−FBS) or presence (+FBS) of serum by m^7GTP Sepharose affinity chromatography (Fig. 6C). In this assay, m^7GTP, which mimics the cap structure at the 5′ ends of mRNA transcripts, is coupled to Sepharose beads and therefore readily purifies eIF4E and eIF4E-associated proteins, such as 4E-BP1, from cell lysate. As expected, WT-4E-BP1 dissociated from eIF4E upon serum stimulation, whereas AA-4E-BP1 remained constitutively bound to eIF4E and did so at higher levels than WT-4E-BP1. The mutant of 4E-BP1 that lacked the eIF4E-binding motif (Y54A) failed to associate with eIF4E. To further confirm that these mutants of 4E-BP1 produce effects on translation, we cotransfected the various 4E-BP1 constructs with a bicistronic vector containing both a GFP reporter gene downstream from the β-globin 5′-UTR, which monitors cap-dependent translation in vivo, and a CAT reporter gene downstream from the encephalomyocarditis virus internal ribosome entry site (IRES), which monitors cap-independent translation in vivo (Fig. 6D) (55). As expected, overexpression of WT-4E-BP1 more strongly repressed cap-dependent translation in the absence of serum than in its presence, and rapamycin treatment of serum-stimulated cells expressing WT-4E-BP1 repressed cap-dependent translation. Compared to vector- or WT-4E-BP1-transfected cells, overexpression of AA-4E-BP1 dominantly repressed cap-dependent translation in both the absence or presence of serum, and binding to eIF4E was required for AA-4E-BP1 to repress cap-dependent translation. Therefore, in our cell system, the phosphorylation site mutant AA-4E-BP1 dominantly inhibits cap-dependent translation through its binding to eIF4E, as expected.

To determine whether mTOR signals independently along both the S6K1 and 4EBP1/eIF4E pathways to control G_1-phase progression, cells were transfected with the AA-4E-BP1 or RNAi-S6K1 plasmids individually or together, and the ability of the cells to enter S-phase after serum stimulation was assayed. Figure 6E clearly shows that although downregulation of each pathway individually inhibited S-phase entry, simulta-

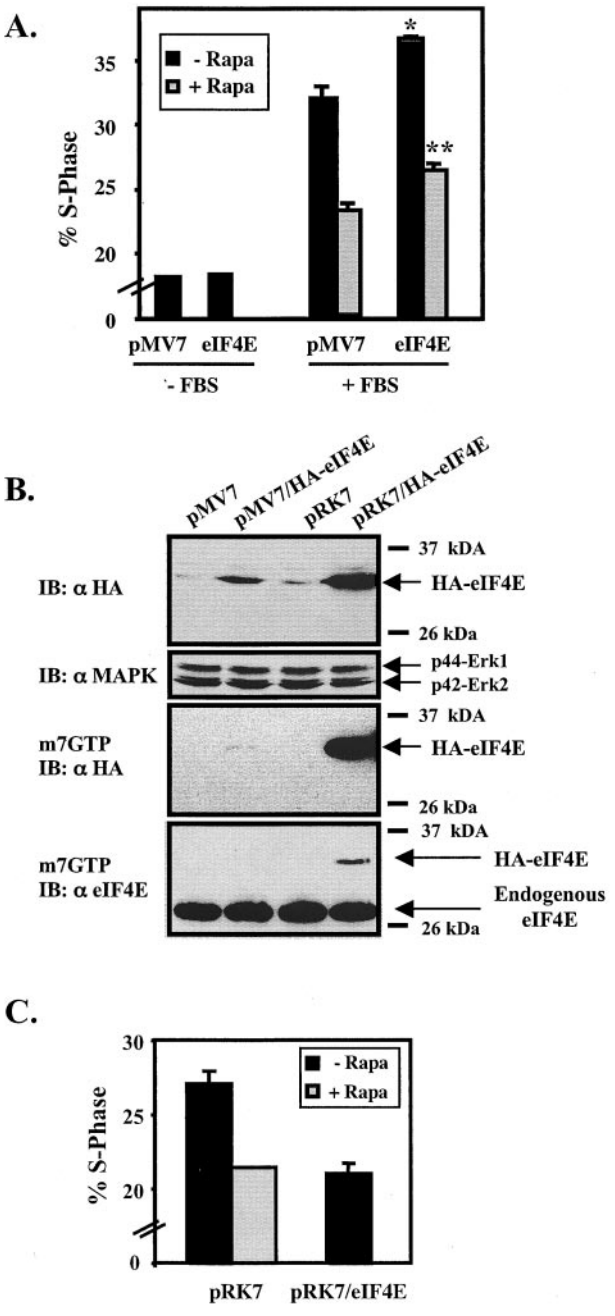

FIG. 5. Overexpression of eIF4E partially rescues rapamycin-inhibited G_1-phase progression and accelerates G_1-phase progression in the absence of drug. (A) Cells were cotransfected with CD20 (1 μg) and either pMV7 vector or HA-eIF4E (expressed from pMV7) (10 μg), serum deprived, and then refed with DMEM/10% FBS in the absence or presence of rapamycin for 20 h. The percentages of $FITC^+$ cells that were in S phase after serum deprivation (−FBS) and of those that entered S phase after 20 h stimulation (+FBS) are shown. ✻, $P = 0.01$ (comparison of pMV7 to eIF4E in the presence of FBS but without rapamycin); ✻✻, $P = 0.004$ (comparison of pMV7 to eIF4E in the presence of both FBS and rapamycin). (B) Vector pRK7 drives expression of eIF4E to much higher levels than vector pMV7. After transfection with vector controls, pMV7/HA-eIF4E, or pRK7/HA-eIF4E plasmids, cells were serum deprived, refed with DMEM–10% FBS for 20 h, and lysed. Protein expression levels were assayed by anti-HA and anti-MAPK (loading control) immunoblotting. Expression of transfected eIF4E (anti-HA blot) and endogenous eIF4E (anti-eIF4E blot) was also determined by m^7GTP Sepharose affinity purification (m^7GTP pull-down) as described in Materials and Methods. (C) Cells were cotransfected with CD20 (1 μg) and either pRK7 vector or eIF4E (expressed from pRK7) (10 μg), serum deprived, and then refed with DMEM–10% FBS in the absence or presence of rapamycin for 20 h. The percentage of cells in S phase after 20 h stimulation is shown.

neous downregulation of both pathways more strongly inhibited S-phase entry to an extent approaching that of rapamycin treatment. Since downregulation of both the eIF4E and S6K1 pathways did not completely mimic rapamycin-mediated inhibition of G_1-phase progression, it is possible that either there exist other mTOR-dependent pathways yet to be identified that contribute to mTOR-dependent cell cycle control or that we have not completely downregulated these pathways. Importantly, coexpression of the dominant AA-4E-BP1 mutant with RR-mTOR blocked the ability of RR-mTOR to restore G_1 progression in the presence of rapamycin, a finding consistent with the idea that 4E-BP1-dependent cell cycle control is mediated by mTOR (data not shown).

Overexpression of S6K1 in C2C12 myoblasts confers a proliferative advantage in low serum-containing media. Lastly, we determined whether overexpression of WT-S6K1 could confer a proliferative advantage in low-serum-containing media, a hallmark of transformation. We therefore generated pools of C2C12 myoblasts stably expressing pMV7 vector control or HA-tagged S6K1. We chose C2C12 cells for two reasons: C2C12 proliferation is particularly rapamycin sensitive, suggesting that the S6K1 pathway may be important for proliferation control in this cell line, and we were unable to generate U2OS lines that stably overexpressed S6K1. In both full-serum-containing media (20% FBS) and low-serum-containing media (2% FBS), total S6K activity was increased ~3-fold in S6K1-expressing pools compared to parental cells or pMV7-expressing pools (Fig. 7A). Surprisingly, total S6K1 activity in 2% FBS was increased ~3-fold across the board relative to total S6K1 activity in 20% FBS, suggesting that low serum activates a positive feedback loop in C2C12 cells that ultimately increases S6K1 activity. In 20% FBS, the extent of phosphorylation of ribosomal protein S6 correlated well with the amount of S6K1 activity; in 2% FBS, however, conditions in which overall S6K1 activity is higher, there was no difference in the extent of phosphorylation of ribosomal protein S6 among the various cell lines, most likely due to the fact that this high level of S6K1 activity is sufficient to fully phosphorylate ribosomal protein S6. After characterizing the stable cell lines, we assayed their ability to proliferate over 6 days in low-serum-containing media (2% FBS). Overexpression of S6K1 clearly conferred a proliferative advantage in low-serum-containing media compared to parental cells or the pMV7 control line; no differences in rates of proliferation were observed in full-serum-containing media (20% FBS) (data not shown) (Fig. 7B). Interestingly, whereas overexpression of WT-S6K1 allowed cells to proliferate in low serum better than controls, this cell line did not exhibit greater S6 phosphorylation. This result may indicate that, similar to what we observed in Fig. 3, phosphorylation of ribosomal protein S6 may not be the critical downstream target of S6K1 that is important for S6K1-dependent cell cycle control. It is important to note that the ability of

S6K1 overexpression to drive proliferation in low serum likely does not result from an inhibition of C2C12 myoblast differentiation, which is normally induced by serum withdrawal. When C2C12 cells are cultured in 2% FBS, they still proliferate, albeit slowly, and do not show any morphological changes characteristic of muscle differentiation. Furthermore, the activity of S6K1 increases during C2C12 differentiation, although it is not required (12) and, indeed, our data (Fig. 6A) clearly confirms that S6K1 is more active in low serum (2% FBS) than in high serum (20% FBS). Therefore, it is unlikely that S6K1 enhances apparent proliferation rate by inhibiting differentiation, and thus the observed proliferation effect is likely to be direct.

DISCUSSION

Although mTOR has been known to control G_1-phase progression, the roles of specific mTOR-dependent pathways in cell cycle control have remained poorly defined. We demonstrate that restoration of mTOR function by using rapamycin-resistant mutant rescues rapamycin-inhibited G_1-phase progression, as in lower eukaryotes (18). This result is consistent with the reported requirement for mTOR in G_1-phase progression; microinjection of the isolated FKBP12-rapamycin-binding (FRB) domain of mTOR inhibited serum-stimulated S-phase entry, presumably by functioning as a dominant-negative (57). Our data furthermore define roles for the mTOR-regulated S6K1 and 4E-BP1/eIF4E pathways in the control of G_1-phase progression by mTOR: activation of either the S6K1 or 4E-BP1/eIF4E pathways partially rescues the inhibitory effect of rapamycin on G_0-to-S-phase cell cycle progression and modestly accelerates cell cycle progression in the absence of drug. mTOR-dependent phosphorylation of 4E-BP1 is required for mTOR's ability to drive the cell cycle, as is the ability of the mTOR/raptor complex to associate with 4E-BP1 via the TOS motif. Both the S6K1 and the 4E-BP1/eIF4E pathways independently mediate mTOR-dependent cell cycle control in parallel, as simultaneous downregulation of these pathways (using RNAi against S6K1 and overexpression of the phosphorylation site mutant AA-4E-BP1) additively inhibits G_1-phase progression compared to downregulation of the pathways individually.

Our finding that RR-S6K1 partially rescues rapamycin-inhibited G_1-phase progression is consistent with previous reports in which RR-S6K1 could partially restore rapamycin-suppressed E2F transcriptional responses in Kit225 cells, a human T-cell line (3), and could partially rescue rapamycin-inhibited proliferation of vascular endothelial cells, as assayed by measuring [^{3}H]thymidine incorporation (58). Importantly, we demonstrate that overexpression of S6K1 accelerates serum-stimulated G_1-phase progression and increases the proliferation rate in low serum, suggesting that the activity of S6K1 is limiting for G_1-phase progression. Since the reduction of S6K1 expression by using RNAi inhibited but did not completely block G_1-phase progression, our data suggest that, although S6K1 participates in cell cycle control, it is not absolutely required for serum-stimulated G_1-phase progression. This result differs from a previous report in which microinjection of anti-S6K1 antibodies blocked serum-stimulated S-phase entry, as well as total protein synthesis and c-Fos induction (26). Although it is possible that the more modest requirement for S6K1 that we demonstrate here results from our inability to completely inhibit S6K1 signaling with RNAi or results from cell type-specific differences, our data demonstrate complete RNAi-mediated reduction of overexpressed S6K1 and phosphorylation of endogenous ribosomal protein S6. Consistent with our data, deletion of S6K1 in embryonic stem cells reduces, but does not block, the capacity of the cells to proliferate in culture, and rapamycin treatment further reduces proliferation rate of these cells (23). Furthermore, rapamycin completely inhibits S6K1 and S6K2 activity, yet only modestly reduces total protein synthesis, does not block serum-stimulated c-Fos induction, and only delays G_1-phase progression. Thus, the formation of intracellular S6K1-containing immune complexes formed by antibody microinjection may disrupt cellular functions differently than the mere absence of S6K1 by RNAi. Collectively, the data suggest that, although it is not absolutely required, S6K1 has a positive influence on cell cycle progression and proliferation and that other mTOR-dependent signaling pathways likely contribute to this as well.

That reduction of S6K1 expression does not induce cell cycle arrest is consistent with our finding that the 4E-BP1/eIF4E pathway operates in parallel to S6K1 downstream of mTOR to control cell cycle progression. We report negative and positive roles for 4E-BP1 and eIF4E, respectively, in control of mTOR-regulated G_1-phase progression in mammalian cells. These data are consistent with transformation of rodent fibroblasts by overexpression of eIF4E (27), which is blocked by cooverexpression of 4E-BP1 (41), and consistent with the increased cell division time caused by antisense RNA-mediated reduction in eIF4E expression (10). Our finding that overexpression of eIF4E accelerates G_1-phase progression appears at first to conflict with a report that eIF4E overexpression activates a negative-feedback loop, resulting in the dephosphorylation of S6K1 and 4E-BP1 (24). It is important to note that eIF4E accelerates the G_1 phase in our cell system when it is expressed at low levels from the weak retroviral long terminal repeat promoter; when eIF4E is expressed to much higher levels with a strong CMV promoter, however, G_1-phase progression is inhibited. Therefore, expression level likely determines whether eIF4E activates a negative feedback loop to restrict aberrant cell cycle progression and proliferation. Since simultaneous downregulation of both the S6K1 and 4E-BP1/eIF4E pathways inhibits G_1-phase progression to an extent approaching that of rapamycin, it is likely that these represent the major pathways mediating mTOR-dependent cell cycle control.

We also consistently noted that the combination of KD mTOR plus rapamycin more strongly inhibits 4E-BP1 phosphorylation, G_1-phase progression, and cell size (13) compared to WT-mTOR plus rapamycin. The trivial explanation for these phenomena is that although rapamycin blocks all mTOR signals, it does so incompletely. A more intriguing possibility is that mTOR also possesses rapamycin-insensitive kinase-dependent functions that, although obviously not inhibited by rapamycin, could be blocked with kinase-inactive and dominant-negative mTOR. In this case, inhibition of the rapamycin-sensitive functions of mTOR by treatment with rapamycin would unmask these rapamycin-insensitive functions of the mTOR kinase. Indeed, the observation that rapamycin completely inhibits S6K1 and endogenous ribosomal prtotein S6

phosphorylation suggests that the blockade of at least some mTOR signals by rapamycin is complete. Furthermore, TOR2 in budding yeast mediates both rapamycin-sensitive and rapamycin-insensitive signals, and one of the proteins (AVO1) found in the rapamycin-insensitive TOR2 complex (TORC2) has a mammalian orthologue of unknown function, mAVO1/hSIN1 (28). Therefore, although the possibility that mTOR may signal in a rapamycin-insensitive manner needs to be investigated much more carefully, there is precedent for the idea.

We reported previously that mTOR controls cell size, which is mediated, at least in part, by the S6K1 and 4E-BP1/eIF4E signaling pathways (13). Since both cell size and cell cycle progression are controlled by mTOR and by the same mTOR-dependent signaling pathways, this nutrient- and mitogen-responsive signaling molecule is centrally positioned to couple cell growth with cell division (Fig. 8A). These data, together with the known dependence of cell cycle progression on a sufficient level of cell growth (22; for a review, see reference 36), suggest a model in which mTOR primarily drives cell growth (i.e., macromolecular biosynthesis), and as a secondary consequence promotes cell cycle progression (Fig. 8B, model 1). Although we favor this model, our data do not exclude the possibility that mTOR controls cell cycle progression via a cell growth-independent mechanism (Fig. 8B model 2); for example, mTOR-dependent signaling could directly regulate components of the cell cycle machinery via a fast-acting phosphorylation cascade. Indeed, the phosphatidylinositol 3-kinase/Akt pathway, which coordinates growth factor signaling with mTOR signals, has been reported to have direct effects on the cell cycle machinery (11, 40, 63).

Our data also show that the increased cell size produced by S6K1 or eIF4E overexpression (13) results from augmented cell growth and not from delayed cell cycle progression. Conversely, the decreased cell size observed upon 4E-BP1 overexpression results from decreased cell growth and not from accelerated cell cycle progression. We make this point because cell size phenotypes can result from changes in either cell growth rate or cell cycle progression rate (e.g., when the cell cycle is blocked, cells grow to increased cell size; when the cell cycle accelerates in the face of an unchanged rate of cell growth, cells become smaller). Therefore, whenever a cell size phenotype is observed, it is important to determine whether it results from altered cell growth or altered rate of cell cycle progression.

If mTOR-regulated cell growth influences the rate of cell cycle progression, it seems reasonable to speculate that, since the S6K1 and 4E-BP1/eIF4E pathways control translation, increased expression of critical cell cycle regulatory proteins could represent a mechanism by which cell cycle progession is coupled to cell growth. Indeed, the synthesis of the G_1-cyclin CLN3 in budding yeast is controlled by TOR and Cdc33 (an eIF4E orthologue) at the level of translation initiation, effectively coupling the synthesis of a cell cycle regulator to protein biosynthetic rate (2). A short upstream open reading frame in the 5′ leader of the CLN3 transcript functions as a translational control element to repress CLN3 expression when protein synthesis and cell growth rate are low (38). Since eIF4E has also been reported to regulate nucleocytoplasmic transport of mRNA transcripts (reviewed in reference 51), it is also possible that eIF4E drives cell growth and cell cycle progres-

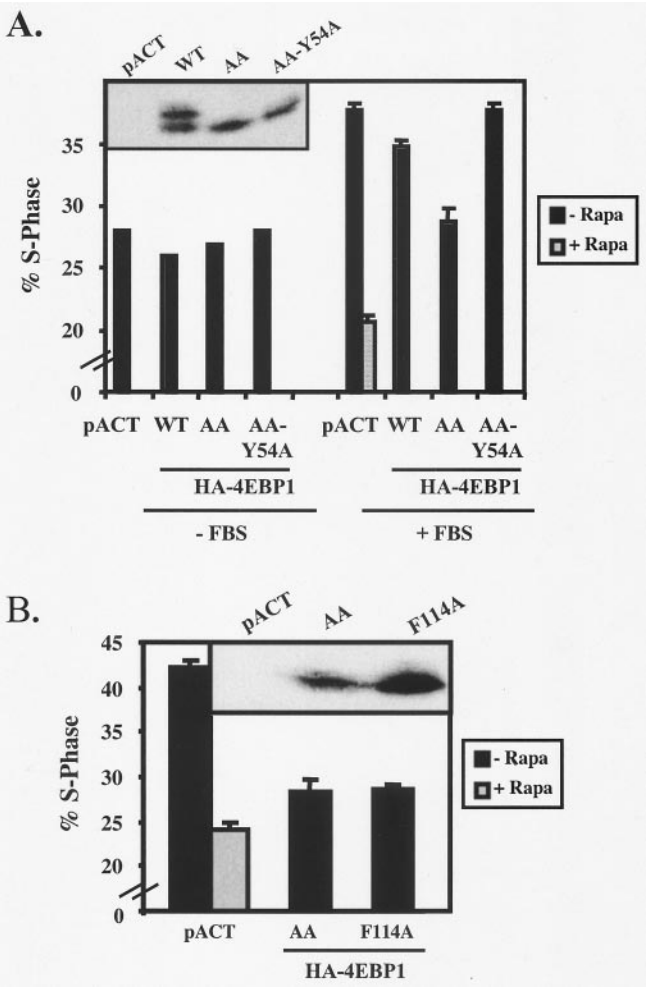

FIG. 6. mTOR-insensitive mutants of 4E-BP1 inhibit G_1-phase progression. Simultaneous downregulation of both the S6K1 and eIF4E pathways additively inhibit G_1-phase progression. (A) Cells were transiently cotransfected with CD20 (1 μg) and various HA-tagged 4E-BP1 plasmids or pACTAG-2 vector control (10 μg). Cells were then serum deprived, refed with DMEM–10% FBS where indicated for 20 h in the absence or presence of rapamycin, and analyzed on a flow cytometer. The percentages of $FITC^+$ cells in S phase after serum deprivation (−FBS) and of cells that have entered S phase after serum stimulation (+FBS) are shown. (B) Same as described in panel A, except cells were cotransfected with pACTAG2 vector control, the phosphorylation site mutant of 4E-BP1 (AA-4E-BP1), or the TOS-motif mutant (F114A-4E-BP1). The percentage of $FITC^+$ cells in S phase after serum stimulation is shown. (C) The phosphorylation site mutant AA-4E-BP1 dominantly binds to eIF4E. Cells were transfected with various HA-tagged 4E-BP1 plasmids (+) or pACTAG-2 vector control (−) (5 μg), serum deprived, refed with DMEM–10% FBS where indicated for 20 h, and lysed. Protein expression levels in the lysate are shown by anti-HA and anti-MAPK (loading control) immunoblotting. m^7GTP Sepharose affinity purifications (m^7GTP pull-downs) were analyzed by immunoblotting with a combination of anti-HA and anti-eIF4E antibodies. (D) The phosphorylation site mutant AA-4E-BP1 dominantly inhibits cap-dependent translation. Cells were cotransfected with a bicistronic plasmid (pGFP/CAT) that directs expression of GFP in a cap-dependent manner (using the β-globin 5′-UTR) and CAT in an IRES-dependent manner (using the encephalomyocarditis virus IRES) (0.5 μg), together with HA-tagged 4E-BP1 plasmids or pACTAG-2 vector control (5 μg). Cells were serum deprived (−FBS), refed with DMEM–10% FBS (+FBS) in the absence or presence of rapamycin, and labeled with [^{35}S]methionine-cysteine. Protein expression in the lysates was assayed by anti-HA and anti-

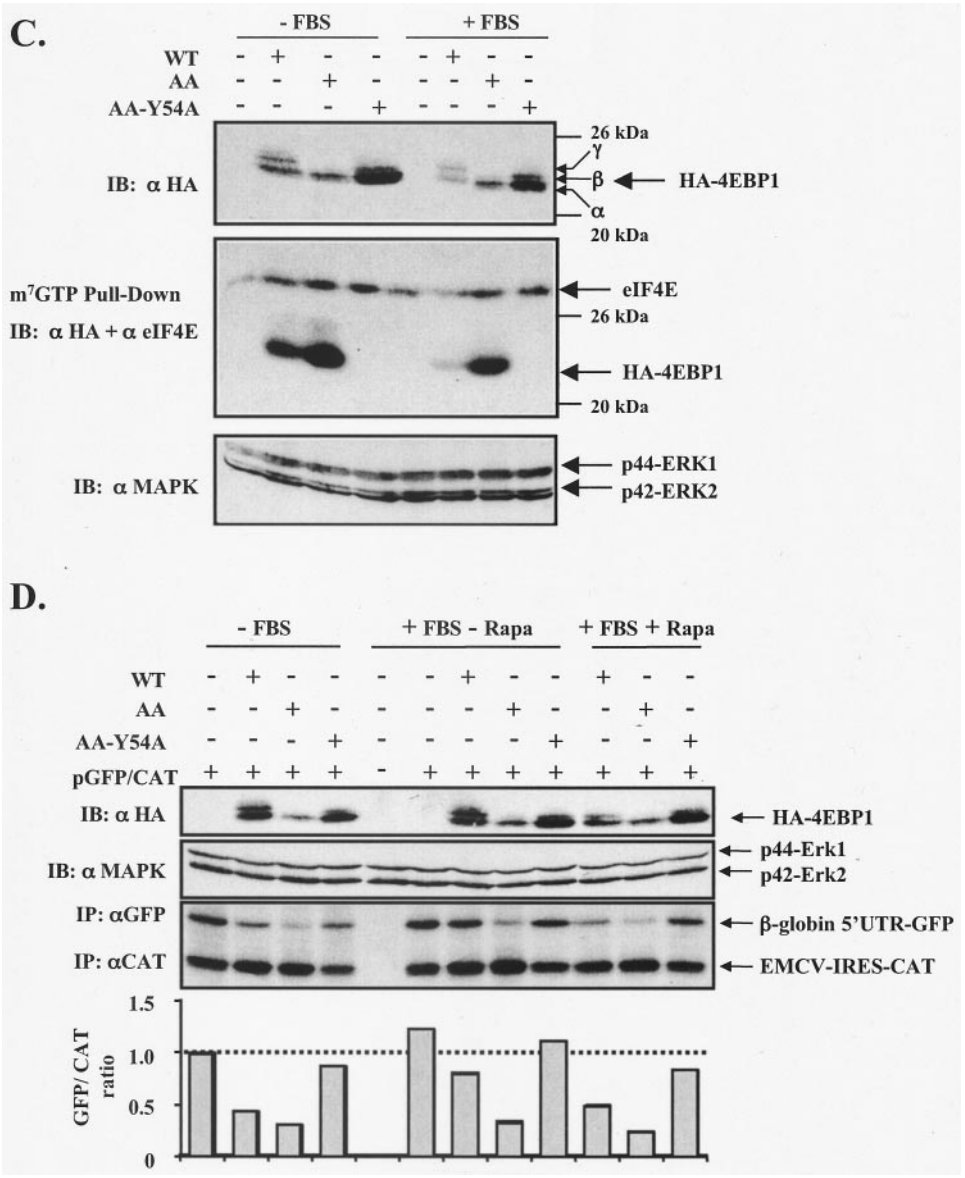

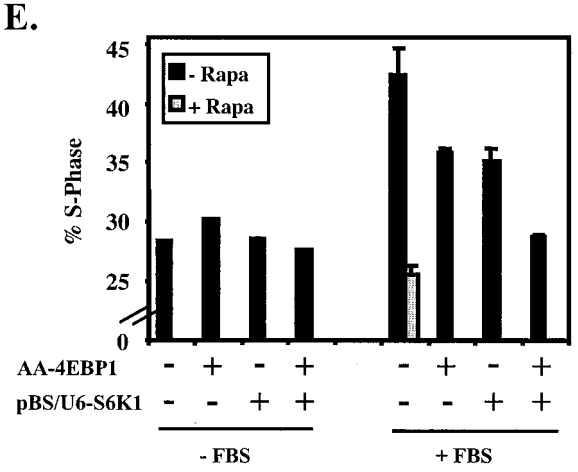

MAPK (loading control) immunoblot- ting, and the expression of ^{35}S-labeled GFP and CAT proteins was assayed by immunoprecipitation and SDS-PAGE (see Materials and Methods). The expression of GFP and CAT was quantitated on a phosphorimager and plotted as the ratio of the GFP signal versus the CAT signal (graph at bottom of panel). (E) Cells were transiently cotransfected with CD20 (1 μg), together with AA-4E-BP1 (5 μg) and pBS/U6-S6K1 (5 μg). Cells were then serum deprived, refed with DMEM–10% FBS where indicated for 20 h in the absence or presence of rapamycin, and analyzed on a flow cytometer. The percentages of FITC$^+$ cells that were in S phase after serum deprivation (−FBS) and of cells that have entered S phase after serum stimulation (+FBS) are shown.

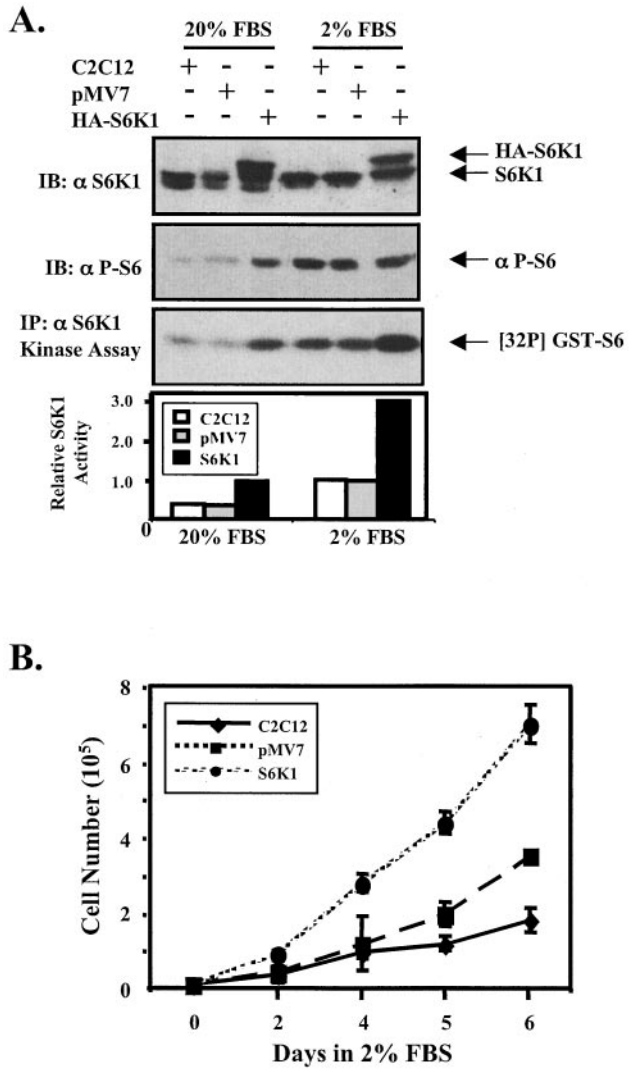

FIG. 7. Overexpression of S6K1 in C2C12 myoblasts confers a proliferative advantage in low-serum-containing media. (A) Parental C2C12 myoblasts or C2C12 cells stably expressing HA-tagged S6K1 or pMV7 vector control as pools were cultured in DMEM containing either 20% (normal serum concentration) or 2% FBS (low serum concentration). Protein expression was assayed by anti-S6K1 and anti-phospho-S6 immunoblotting. Kinase activity was assayed by anti-S6K1 immune complex assay with GST-S6 as a substrate. (B) Equal numbers of parental, pMV7, or S6K1-overexpressing C2C12 cells were plated at day 0 in DMEM–2% FBS, and cell numbers were determined at days 2, 4, 5, and 6.

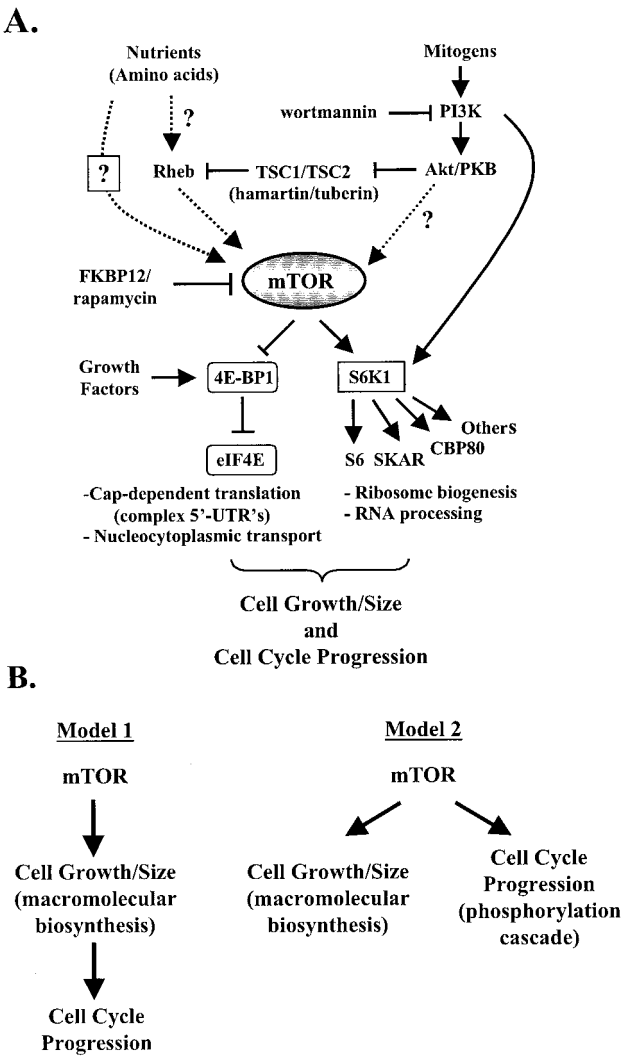

FIG. 8. Models. (A) mTOR functions as a central coordinator of mTOR-dependent cell growth/cell size and cell cycle progression. The mTOR kinase regulates at least two downstream signaling pathways, the S6K1 and 4E-BP1/eIF4E pathways, that promote (i) cell growth and/or size and (ii) cell cycle progression when sufficient amounts of nutrients and mitogens are present. How nutrients regulate mTOR is poorly understood. Rheb was recently identified as a positive upstream regulator of mTOR that likely integrates nutrient and mitogen signals. The TSC1/TSC2 tuberous sclerosis complex (hamartin/tuberin) functions as a tumor suppressor to inhibit mTOR-dependent signaling in the absence of sufficient mitogens via inactivation of Rheb through the GAP activity of TSC2 (tuberin). Growth factors, via Akt/PKB-dependent phosphorylation of TSC2, inhibit the repressive action of the TSC1/TSC2 complex on Rheb, thus promoting mTOR-dependent signaling. (B) Models describing how mTOR couples cell growth and cell cycle progression. In model 1, mTOR primarily controls cell growth and/or cell size through macromolecular biosynthetic processes (i.e., translation) and, as a secondary consequence, regulates the rate of cell cycle progression. In model 2, mTOR regulates (i) cell growth and/or size and (ii) cell cycle progression through distinct mechanisms, such as through macromolecular biosynthetic processes and phosphorylation cascades, respectively.

sion by increasing the nucleocytoplasmic export rate of mRNAs encoding specific cell cycle regulators instead of or in addition to controlling their translation. Although the identity of the critical eIF4E-controlled cell cycle regulator(s) is not known at this time, eIF4E has been shown to increase the translation of ODC and c-Myc and to increase the expression of cyclin D1 through increased nucleocytoplasmic transport (42; reviewed in reference 48).

The mechanism by which S6K1 drives cell growth and the cell cycle is also unclear. Of course, S6K1-dependent phosphorylation of ribosomal protein S6 may drive ribosome biogenesis and therefore increase protein biosynthetic capacity, resulting in augmented cell growth and promotion of cell cycle progression. Although S6K1 clearly controls cell growth and cell cycle progression, the critical downstream targets respon-

sible for mediating this response are not clearly defined. In two different experiments with two different cell types, we noted that the degree of ribosomal protein S6 phosphorylation was not concordant with the cell cycle phenotype produced by S6K1 overexpression. For example, the S6K1 mutants $E_{389}D_3E$ and $E_{389}\Delta CT$ accelerated G_1-phase progression, whereas WT-S6K1 did not, and yet overexpression of all three S6K1 constructs increased the phosphorylation of ribosomal protein S6 over vector control. In addition, S6K1 overexpression increased proliferation rate in low serum compared to parental or control cells, and yet in low serum ribosomal protein S6 was phosphorylated to similar levels in all three cell lines. The observation that S6K1-regulated G_1-phase progression and ribosomal protein S6 phosphorylation can be dissociated suggests the intriguing possibility that S6K1 likely has other targets besides the ribosomal protein S6. Consistent with this idea, we have recently identified a novel S6K1-interacting protein and in vivo substrate, SKAR, which bears homology to the ALY/REF family of proteins that couple transcription, splicing, and RNA export (C. Richardson et al., unpublished data). SKAR also controls cell growth or cell size and also regulates the rate of cell cycle progression (Richardson et al., unpublished), suggesting that S6K1 may control cell growth and cell cycle progression through an RNA processing event (Fig. 8A). Another in vivo target of S6K1 is the cap-binding protein CBP80, which functions in an early step of RNA splicing (60). Therefore, it is possible that S6K1-regulated cell cycle progression may be due in part to regulation of RNA processing (Fig. 8A). Alternatively, S6K1 could regulate the cell cycle by a cell growth-independent mechanism via phosphorylation of unidentified targets that would directly regulate the cell cycle machinery (Fig. 8B, model 2).

In the present study, we identify the S6K1 and 4E-BP1/eIF4E pathways as the major mTOR-dependent downstream signaling pathways that mediate mTOR-regulated G_1-phase progression (Fig. 8A). Since these pathways also mediate mTOR-dependent control of cell growth or cell size (13), mTOR is uniquely positioned to function as a central coordinator of cell growth and cell division. In the future, we hope to better understand the relationship between mTOR-regulated cell growth and cell division and to move further downstream to determine how mTOR couples these fundamental biological processes.

ACKNOWLEDGMENTS

We thank Robert Abraham for his generous donation of mTOR plasmids, Nahum Sonenberg for generously sharing the eIF4E and 4E-BP1 plasmids, Morris Birnbaum for generously providing the anti-phospo-S6 antibodies, and A. A. M. Thomas for sharing the pGFP/CAT plasmid. We are grateful to Martin G. Myers, Jr., for critical reading of the manuscript and members of the Blenis lab for help in general, particularly Stefanie Schalm for generating the pACTAG2/3HA-AA-Y54A-4E-BP1 mutant. We especially thank Jennifer Waters-Shuler and the Nikon Imaging Center at Harvard Medical School for help with immunofluorescence image training and acquisition.

We thank the Tuberous Sclerosis (TS) Alliance and the Rothberg Courage Fund. This study was supported by an NIH award GM51405 to J.B. D.C.F. was supported by NIH NRSA fellowship F32 CA69808 and by the TS Alliance, C.R. was supported by NCI grant T32 CA09361, and A.T. was supported by ALT2002-463.

REFERENCES

1. **Abraham, R. T., and G. J. Wiederrecht.** 1996. Immunopharmacology of rapamycin. Annu. Rev. Immunol. **14:**483–510.
2. **Barbet, N. C., U. Schneider, S. B. Helliwell, I. Stansfield, M. F. Tuite, and M. N. Hall.** 1996. TOR controls translation initiation and early G_1 progression in yeast. Mol. Biol. Cell **7:**25–42.
3. **Brennan, P., J. W. Babbage, G. Thomas, and D. Cantrell.** 1999. $p70^{s6k}$ integrates phosphatidylinositol 3-kinase and rapamycin-regulated signals for E2F regulation in T lymphocytes. Mol. Cell. Biol. **19:**4729–4738.
4. **Brown, E. J., P. A. Beal, C. T. Keith, J. Chen, T. B. Shin, and S. L. Schreiber.** 1995. Control of p70 S6 kinase by kinase activity of FRAP in vivo. Nature **377:**441–446.
5. **Brunn, G. J., C. C. Hudson, A. Sekulic, J. M. Williams, H. Hosoi, P. J. Houghton, J. C. Lawrence, Jr., and R. T. Abraham.** 1997. Phosphorylation of the translational repressor PHAS-I by the mammalian target of rapamycin. Science **277:**99–101.
6. **Cheatham, L., M. Monfar, M. M. Chou, and J. Blenis.** 1995. Structural and functional analysis of p70 S6 kinase. Proc. Natl. Acad. Sci. USA **92:**11696–11700.
7. **Chen, R.-H., C. Sarnecki, and J. Blenis.** 1992. Nuclear localization and regulation of the erk- and rsk-encoded protein kinases. Mol. Cell. Biol. **12:**915–927.
8. **Choi, K. M., L. P. McMahon, and J. C. Lawrence, Jr.** 2003. Two motifs in the translational repressor PHAS-I required for efficient phosphorylation by mammalian target of rapamycin and for recognition by Raptor. J. Biol. Chem. **278:**19667–19673.
9. **Crespo, J. L., and M. N. Hall.** 2002. Elucidating TOR signaling and rapamycin action: lessons from *Saccharomyces cerevisiae*. Microbiol. Mol. Biol. Rev. **66:**579–591.
10. **De Benedetti, A., S. Joshi-Barve, C. Rinker-Schaeffer, and R. E. Rhoads.** 1991. Expression of antisense RNA against initiation factor eIF-4E mRNA in HeLa cells results in lengthened cell division times, diminished translation rates, and reduced levels of both eIF-4E and the p220 component of eIF-4F. Mol. Cell. Biol. **11:**5435–5445.
11. **Diehl, J. A., M. Cheng, M. F. Roussel, and C. J. Sherr.** 1998. Glycogen synthase kinase-3β regulates cyclin D1 proteolysis and subcellular localization. Genes Dev. **12:**3499–3511.
12. **Erbay, E., and J. Chen.** 2001. The mammalian target of rapamycin regulates C2C12 myogenesis via a kinase-independent mechanism. J. Biol. Chem. **276:**36079–36082.
13. **Fingar, D. C., S. Salama, C. Tsou, E. Harlow, and J. Blenis.** 2002. Mammalian cell size is controlled by mTOR and its downstream targets S6K1 and 4EBP1/eIF4E. Genes Dev. **16:**1472–1487.
14. **Garami, A., F. J. T. Zwartkruis, T. Nobukuni, M. Joaquin, M. Roccio, H. Stocker, S. Kozma, E. Hafen, J. L. Bos, and G. Thomas.** 2003. Insulin activation of Rheb, a mediator of mTOR/S6K/4E-BP signaling, is inhibited by TSC1 and 2. Mol. Cell **11:**1457–1466.
15. **Gingras, A. C., B. Raught, and N. Sonenberg.** 2001. Regulation of translation initiation by FRAP/mTOR. Genes Dev. **15:**807–826.
16. **Hara, K., Y. Maruki, X. Long, K. Yoshino, N. Oshiro, S. Hidayat, C. Tokunaga, J. Avruch, and K. Yonezawa.** 2002. Raptor, a binding partner of target of rapamycin (TOR), mediates TOR action. Cell **110:**177–189.
17. **Hara, K., K. Yonezawa, M. T. Kozlowski, T. Sugimoto, K. Andrabi, Q. P. Weng, M. Kasuga, I. Nishimoto, and J. Avruch.** 1997. Regulation of eIF-4E BP1 phosphorylation by mTOR. J. Biol. Chem. **272:**26457–26463.
18. **Heitman, J., N. R. Mowa, and M. N. Hall.** 1991. Targets for cell cycle arrest by the immunosuppressant rapamycin in yeast. Science **253:**905–909.
19. **Jacinto, E., and M. N. Hall.** 2003. Tor signalling in bugs, brain and brawn. Nat. Rev. Mol. Cell. Biol. **4:**117–126.
20. **Jefferies, H. B., S. Fumagalli, P. B. Dennis, C. Reinhard, R. B. Pearson, and G. Thomas.** 1997. Rapamycin suppresses 5′TOP mRNA translation through inhibition of p70s6k. EMBO J. **16:**3693–3704.
21. **Jefferies, H. B. J., C. Reinhard, S. C. Kozma, and G. Thomas.** 1994. Rapamycin selectively represses translation of the "polypryimidine tract" nRNA family. Proc. Natl. Acad. Sci. USA **91:**4441–4445.
22. **Johnston, G. C., J. R. Pringle, and L. H. Hartwell.** 1977. Coordination of growth with cell division in the yeast *Saccharomyces cerevisiae*. Exp. Cell Res. **105:**79–98.
23. **Kawasome, H., P. Papst, S. Webb, G. M. Keller, G. L. Johnson, E. W. Gelfand, and N. Terada.** 1998. Targeted disruption of $p70^{s6k}$ defines its role in protein synthesis and rapamycin sensitivity. Proc. Natl. Acad. Sci. USA **95:**5033–5038.
24. **Khaleghpour, K., S. Pyronnet, A. C. Gingras, and N. Sonenberg.** 1999. Translational homeostasis: eukaryotic translation initiation factor 4E control of 4E-binding protein 1 and p70 S6 kinase activities. Mol. Cell. Biol. **19:**4302–4310.
25. **Kim, D. H., D. D. Sarbassov, S. M. Ali, J. E. King, R. R. Latek, H. Erdjument-Bromage, P. Tempst, and D. M. Sabatini.** 2002. mTOR interacts with raptor to form a nutrient-sensitive complex that signals to the cell growth machinery. Cell **110:**163–175.

26. **Lane, H. A., A. Fernandez, N. J. C. Lamb, and G. Thomas.** 1993. $p70^{S6k}$ function is essential for G_1 progression. Nature **363:**170–172.
27. **Lazaris-Karatzas, A., K. S. Montine, and N. Sonenberg.** 1990. Malignant transformation by a eukaryotic initiation factor subunit that binds to mRNA 5′ cap. Nature **345:**544–547.
28. **Loewith, R., E. Jacinto, S. Wullschleger, A. Lorberg, J. L. Crespo, D. Bonenfant, W. Oppliger, P. Jenoe, and M. N. Hall.** 2002. Two TOR complexes, only one of which is rapamycin sensitive, have distinct roles in cell growth control. Mol. Cell **10:**457–468.
29. **Martin, K. A., and J. Blenis.** 2002. Coordinate regulation of translation by the PI 3-kinase and mTOR pathways. Adv. Cancer Res. **86:**1–39.
30. **Martin, K. A., S. S. Schalm, C. Richardson, A. Romanelli, K. L. Keon, and J. Blenis.** 2001. Regulation of ribosomal S6 kinase 2 by effectors of the phosphoinositide 3-kinase pathway. J. Biol. Chem. **276:**7884–7891.
31. **McManus, E. J., and D. R. Alessi.** 2002. TSC1-TSC2: a complex tale of PKB-mediated S6K regulation. Nat. Cell Biol. **4:**E214–E216.
32. **Neufeld, T. P., A. F. de la Cruz, L. A. Johnston, and B. A. Edgar.** 1998. Coordination of growth and cell division in the *Drosophila* wing. Cell **93:**1183–1193.
33. **Nojima, H., C. Tokunaga, S. Eguchi, N. Oshiro, S. Hidayat, K. Yoshino, K. Hara, N. Tanaka, J. Avruch, and K. Yonezawa.** 2003. The mammalian target of rapamycin (mTOR) partner, raptor, binds the mTOR substrates p70 S6 kinase and 4E-BP1 through their TOR signaling (TOS) motif. J. Biol. Chem. **278:**15461–15464.
34. **Oldham, S., and E. Hafen.** 2003. Insulin/IGF and target of rapamycin signaling: a TOR de force in growth control. Trends Cell Biol. **13:**79–85.
35. **Oldham, S., J. Montagne, T. Radimerski, G. Thomas, and E. Hafen.** 2000. Genetic and biochemical characterization of dTOR, the *Drosophila* homolog of the target of rapamycin. Genes Dev. **14:**2689–2694.
36. **Pardee, A. B.** 1989. G_1 events and regulation of cell proliferation. Science **246:**603–608.
37. **Pearson, R. B., P. B. Dennis, J. W. Han, N. A. Williamson, S. C. Kozma, R. E. Wettenhall, and G. Thomas.** 1995. The principal target of rapamycin-induced $p70^{S6k}$ inactivation is a novel phosphorylation site within a conserved hydrophobic domain. EMBO J. **14:**5279–5287.
38. **Polymenis, M., and E. V. Schmidt.** 1997. Coupling of cell division to cell growth by translational control of the G_1 cyclin CLN3 in yeast. Genes Dev. **11:**2522–2531.
39. **Rohde, J., J. Heitman, and M. E. Cardenas.** 2001. The TOR kinases link nutrient sensing to cell growth. J. Biol. Chem. **276:**9583–9586.
40. **Rossig, L., A. S. Jadidi, C. Urbich, C. Badorff, A. M. Zeiher, and S. Dimmeler.** 2001. Akt-dependent phosphorylation of $p21^{Cip1}$ regulates PCNA binding and proliferation of endothelial cells. Mol. Cell. Biol. **21:**5644–5657.
41. **Rousseau, D., A. C. Gingras, A. Pause, and N. Sonenberg.** 1996. The eIF4E-binding proteins 1 and 2 are negative regulators of cell growth. Oncogene **13:**2415–2420.
42. **Rousseau, D., R. Kaspar, I. Rosenwald, L. Gehrke, and N. Sonenberg.** 1996. Translation initiation of ornithine decarboxylase and nucleocytoplasmic transport of cyclin D1 mRNA are increased in cells overexpressing eukaryotic initiation factor 4E. Proc. Natl. Acad. Sci. USA **93:**1065–1070.
43. **Saucedo, L. J., X. Gao, D. A. Chiarelli, L. Li, D. Pan, and B. A. Edgar.** 2003. Rheb promotes cell growth as a component of the insulin/TOR signalling network. Nat. Cell Biol. **5:**566–571.
44. **Schalm, S. S., and J. Blenis.** 2002. Identification of a conserved motif required for mTOR signaling. Curr. Biol. **12:**632–639.
45. **Schalm, S. S., D. C. Fingar, D. M. Sabatini, and J. Blenis.** 2003. TOS motif-mediated Raptor binding regulates 4E-BP1 multisite phosphorylation and function. Curr. Biol. **13:**797–806.
46. **Schmelzle, T., and M. N. Hall.** 2000. TOR, a central controller of cell growth. Cell **103:**253–262.
47. **Shima, H., M. Pende, Y. Chen, S. Fumagalli, G. Thomas, and S. C. Kozma.** 1998. Disruption of the $p70^{s6k}/p85^{s6k}$ gene reveals a small mouse phenotype and a new functional S6 kinase. EMBO J. **17:**6649–6659.
48. **Sonenberg, N., and A. C. Gingras.** 1998. The mRNA 5′ cap-binding protein eIF4E and control of cell growth. Curr. Opin. Cell Biol. **10:**268–275.
49. **Stocker, H., T. Radimerski, B. Schindelholz, F. Wittwer, P. Belawat, P. Daram, S. Breuer, G. Thomas, and E. Hafen.** 2003. Rheb is an essential regulator of S6K in controlling cell growth in *Drosophila*. Nat. Cell Biol. **5:**559–566.
50. **Stolovich, M., H. Tang, E. Hornstein, G. Levy, R. Cohen, S. S. Bae, M. J. Birnbaum, and O. Meyuhas.** 2002. Transduction of growth or mitogenic signals into translational activation of TOP mRNAs is fully reliant on the phosphatidylinositol 3-kinase-mediated pathway but requires neither S6K1 nor rpS6 phosphorylation. Mol. Cell. Biol. **22:**8101–8113.
51. **Strudwick, S., and K. L. Borden.** 2002. The emerging roles of translation factor eIF4E in the nucleus. Differentiation **70:**10–22.
52. **Sui, G., C. Soohoo, B. Affar el, F. Gay, Y. Shi, and W. C. Forrester.** 2002. A DNA vector-based RNAi technology to suppress gene expression in mammalian cells. Proc. Natl. Acad. Sci. USA **99:**5515–5520.
53. **Tang, H., E. Hornstein, M. Stolovich, G. Levy, M. Livingstone, D. Templeton, J. Avruch, and O. Meyuhas.** 2001. Amino acid-induced translation of TOP mRNAs is fully dependent on phosphatidylinositol 3-kinase-mediated signaling, is partially inhibited by rapamycin, and is independent of S6K1 and rpS6 phosphorylation. Mol. Cell. Biol. **21:**8671–8683.
54. **Tee, A. R., B. D. Manning, P. P. Roux, L. C. Cantley, and J. Blenis.** 2003. Tuberous sclerosis complex gene products, Tuberin and Hamartin, control mTOR signaling by acting as a GTPase-activating protein complex toward Rheb. Curr. Biol. **13:**1259–1268.
55. **Tee, A. R., and C. G. Proud.** 2002. Caspase cleavage of initiation factor 4E-binding protein 1 yields a dominant inhibitor of cap-dependent translation and reveals a novel regulatory motif. Mol. Cell. Biol. **22:**1674–1683.
56. **Terada, N., H. R. Patel, K. Takase, K. Kohno, A. C. Nairn, and E. W. Gelfand.** 1994. Rapamycin selectively inhibits translation of mRNAs encoding elongation factors and ribosomal proteins. Proc. Natl. Acad. Sci. USA **91:**11477–11481.
57. **Vilella-Bach, M., P. Nuzzi, Y. Fang, and J. Chen.** 1999. The FKBP12-rapamycin-binding domain is required for FKBP12-rapamycin-associated protein kinase activity and G_1 progression. J. Biol. Chem. **274:**4266–4272.
58. **Vinals, F., J. C. Chambard, and J. Pouyssegur.** 1999. p70 S6 kinase-mediated protein synthesis is a critical step for vascular endothelial cell proliferation. J. Biol. Chem. **274:**26776–26782.
59. **Wang, X., W. Li, J. L. Parra, A. Beugnet, and C. G. Proud.** 2003. The C terminus of initiation factor 4E-binding protein 1 contains multiple regulatory features that influence its function and phosphorylation. Mol. Cell. Biol. **23:**1546–1557.
60. **Wilson, K. F., W. J. Wu, and R. A. Cerione.** 2000. Cdc42 stimulates RNA splicing via the S6 kinase and a novel S6 kinase target, the nuclear cap-binding complex. J. Biol. Chem. **275:**37307–37310.
61. **Zhang, H., J. P. Stallock, J. C. Ng, C. Reinhard, and T. P. Neufeld.** 2000. Regulation of cellular growth by the *Drosophila* target of rapamycin dTOR. Genes Dev. **14:**2712–2724.
62. **Zhang, Y., X. Gao, L. J. Saucedo, B. Ru, B. A. Edgar, and D. Pan.** 2003. Rheb is a direct target of the tuberous sclerosis tumour suppressor proteins. Nat. Cell Biol. **5:**578–581.
63. **Zhou, B. P., Y. Liao, W. Xia, B. Spohn, M. H. Lee, and M. C. Hung.** 2001. Cytoplasmic localization of $p21^{Cip1/WAF1}$ by Akt-induced phosphorylation in HER-2/neu-overexpressing cells. Nat. Cell Biol. **3:**245–252.